NUCLEAR SCIENCE AND ENGINEERING: 46, 88-111 (1971)

Optimal Control Rod Programming of Light Water Reactors in Equilibrium Fuel Cycle

Hiroshi Motoda

Atomic Energy Research Laboratory, Hitachi Ltd.
Ozenji, Kawasaki, Kanagawa Pref., Japan

Received December 3, 1970
Revised March 17, 1971

A generalized treatment for investigating the effects of various refueling schemes on the optimal control rod programming that maximizes the average burnup of discharged fuels in a two-region, radially one-dimensional light water moderated nuclear reactor is presented and applied to a boiling water reactor having uranium fuel of a single ^{235}U enrichment. It is assumed that the refueling scheme has reached an equilibrium fuel cycle, and the analysis by burnup space is applied, which helps in interpreting geometrically the coupled effect of the control rod programming and the fuel burnup by the trajectory drawn in this space. Three refueling schemes are considered: parallel, series out-in, and series in-out. Scatter loading is assumed in each region and the batch number and volume fraction of each region are varied as the refueling parameters.

Fuel management and poison management constitute a hierarchy relation, and the effect of the refueling schemes on burnup maximization or enrichment minimization is several times greater than that of the control rod programmings. However, the policy of the optimal control rod programming strongly depends on the refueling scheme. The power density of the inner region should be as high as possible for out-in scheme (inner high policy) and vice versa for in-out scheme (outer high policy). However, either policy can be optimal, depending on the refueling parameters for parallel schemes, and in some cases the optimal control rod programming is not unique (degenerate policy). Optimal control rod programming increases the discharge burnup or decreases the enrichment of the feed fuels by about 0 to 4% over the conventional constant power shape operation. The difference is mainly determined by the reactor design and the refueling scheme. Optimal refueling should be chosen from among parallel schemes, which have much larger freedom than series schemes.

I. INTRODUCTION

The development of nuclear engineering has come to the stage at which nuclear power production is economically competitive with power production by conventional fossil fuels. Thus, effective use of nuclear fuels is becoming more and more important. In bringing this about, modern control theory has been applied to the optimization of fuel management and poison management.

Wall and Fenech[1] showed that an alternative to a dynamic programming algorithm[2] could be applied to the refueling decision of a single enrichment, three-zone 1000-MW(e) pressurized water reactor (PWR) core, in which the optimal decision on the replacement and shuffling of three fuel zones was determined to minimize the power generating cost calculated by the absolute method.

Stover and Sesonske[3] used this same technique,

[1] I. WALL and H. FENECH, *Nucl. Sci. Eng.*, **22**, 285 (1965).

[2] R. E. BELLMAN and S. E. DREYFUS, *Applied Dynamic Programming*, Princeton University Press, Princeton, New Jersey (1962).

[3] R. L. STOVER and A. SESONSKE, *J. Nucl. Energy*, **23**, 673 (1969).

which was shown to be a computational acceleration method of an exhaustive search called "elimination of similar end states", for determining fresh fuel loading decisions which lead to a minimum fuel cost in a scatter-loaded three-zone 1000-MW(e) boiling water reactor (BWR) core.

Fagen and Sesonske[4] used a direct search to determine optimal loading patterns in a scatter-loading PWR core with fuel shuffling between zones. A minimum fuel cycle cost was obtained by determining shuffle patterns that maximized the core life at each reload point in the life of the reactor, assuming a constant fraction of replacement in a 19-zone core which was in a quasi-equilibrium cycle.

Mélice[5] presented a new method for optimal core management for a PWR chemical shim reactor for finding the enrichment of the fresh fuel and the patterns of the various assemblies in the core in the light of the minimum critical mass problem; he applied it to the analysis of the stationary and transient cycles of the SENA reactor, with a three-region mixed reload mode.

Tabak[6] used linear and quadratic programming[7,8] in a simplified one-point reactor model to determine the optimum ^{235}U mass loading which minimized ^{235}U usage or maximized the ^{239}Pu mass removed from the core over the life of the reactor.

The author[9] showed that the variational method can be applied to the burnup optimization of continuous scattered refueling.

No problem of poison management arose in Refs. 5 and 9 in which the chemical shim control and on-power refueling were employed, respectively. However, the optimization of poison management was not considered in any of the other four studies and uniform control was assumed because it was thought that the poison management had weak interactions with and could be separated from fuel management.

Terney and Fenech[10] applied dynamic programming and direct flux synthesis to the space-time optimization problem of determining the optimum sequence of control rod motions in a representative PWR, which minimized the maximum power peaking throughout the life of the reactor.

Suzuki and Kiyose[11] showed that the maximum principle[12] could be applied to the control rod programming optimization that maximized the core life under the constraints of a maximum allowable power-peaking factor and control rod density.

The author[13] tried to interpret geometrically the relations among criticality, power and control rod distribution, and fuel burnup in the burnup space, assuming that one quantity for each region is sufficient to represent a state of a reactor. Optimal control rod programming was obtained for both the radial and the axial directions in a two-region BWR by one-dimensional analyses using the maximum principle.

No consideration was given to fuel management in these three studies. It was tacitly recognized that it was best to maximize the core-averaged burnup or to minimize the maximum power peaking during each refueling interval. Fuel management and poison management constitute a hierarchy relation, and it may be true that the effect of the latter on the former is small. However, the inverse in not true, because the way in which the particular fuels stay in and are discharged from the core is different for each particular refueling scheme. Therefore, the problem of control rod programming optimization cannot be defined unless the refueling scheme is specified when the maximization of the average burnup is desired.

The aim of this paper is to investigate the effect of various refueling schemes on the optimal policy of control rod programming that maximizes the average burnup of discharged fuels within the constraint of a given maximum allowable power-peaking factor in light water moderated reactors. The results of both Wall and Stover indicate that the true equilibrium is not established in an optimum fuel management; rather, a cyclic equilibrium condition is established, which means that the optimal control rod policy may vary from stage to stage. To facilitate treatment, it is assumed that the refueling scheme has reached a true equilibrium cycle.

Three refueling schemes are considered. These are parallel, series out-in, and series in-out schemes. Scatter loading and appropriate fuel shuffling are assumed in each region, and the

[4] J. R. FAGEN and A. SESONSKE, *J. Nucl. Energy*, **23**, 683 (1969).

[5] M. MÉLICE, *Nucl. Sci. Eng.*, **37**, 451 (1969).

[6] D. TABAK, "Optimization of Nuclear Reactor Fuel Recycle via Linear and Quadratic Programming," *Trans. IEEE on Nuclear Science*, NS-**15**, 60 (1968).

[7] G. HADLEY, *Linear Programming*, Addison Wesley Publishing Company, Inc., New York (1962).

[8] G. HADLEY, *Nonlinear and Dynamic Programming*, Addison Wesley Publishing Company, Inc., New York (1964).

[9] H. MOTODA, *Nucl. Sci. Eng.*, **41**, 1 (1970).

[10] W. B. TERNEY and H. FENECH, *Nucl. Sci. Eng.*, **39**, 109 (1970).

[11] A. SUZUKI and R. KIYOSE, *Trans. Am. Nucl. Soc.*, **11**, 441 (1968).

[12] L. S. PONTRYAGIN, V. G. BOLTYANSKII, R. V. GAMKRELIDZE, and E. F. MISHCHENKO, *The Mathematical Theory of Optimal Processes*, Interscience Publishers, New York (1962).

[13] H. MOTODA and T. KAWAI, *Nucl. Sci. Eng.*, **39**, 114 (1970).

batch number (integer) or the inverse refueling fraction and the volume fraction are varied as the refueling parameters.

It was proved that the original problem of burnup maximization is equivalent to that of minimization of enrichment of feed fuels, which makes it possible to satisfy the current operational requirement of a one-year refueling interval. This comes from the need for annual maintenance of a reactor when refueling is performed.

The analysis by burnup space was applied to a two-region BWR core of a single ^{235}U enrichment within the validity of a one-dimensional one-group neutron diffusion equation; the results were compared with the conventional constant power-shape operation.

II. REACTOR MODEL

The following assumptions and approximations were made to represent the characteristics of a single-enrichment two-region BWR.

1. The reactor is cylindrically one-dimensional and the core is divided into two homogenized regions surrounded by a reflector.
2. Neutron distribution is described by a modified one-group neutron diffusion equation and the slowing down property is uniform throughout the core.
3. Neutron flux, averaged over each region, is used to calculate fuel burnup; thus, fuel burnup is assumed uniform in each region.
4. Criticality is maintained by the control rods uniformly distributed in each region.
5. Two types of reactivity feedback are considered, xenon and Doppler. Their power dependence is of the form adopted in the FLARE code.[14] The space dependence of the reactivity feedback of a void is omitted and the nuclear characteristics of the average void are used for the radial analysis.
6. The maximum allowable gross power-peaking factor is given by the reactor design and is used as the operational constraint. No limitations on the local power peaking vs exposure are considered.
7. No limitation on the minimum critical heat flux ratio (MCHFR) is considered. This constraint is assumed to be replaced by assumption 6.

[14]D. L. DELP, D. L. FISHER, J. M. HARRIMAN, and M. J. STEDWELL, "FLARE—A Three-Dimensional Boiling Water Reactor Simulator," GEAP-4598, General Electric Company (1964).

To satisfy assumptions 1, 3, and 6, extensive intra-region fuel shuffling is required, which, in many cases, could be undesirable. However, interchange of the rod patterns will help rationalize assumption 4. For assumption 7, MCHFR and the maximum allowable power peak do not necessarily coincide in a given BWR. MCHFR could be more restrictive than the allowable peak. However, as long as only radial peaking is considered and the axial shape is assumed fixed, the restriction on peaking is probably reasonable. All these assumptions limit the usefulness of the present study in actual design practice but are necessary for the present model.

The two-group neutron diffusion equation without reactivity feedbacks is written in one-dimensional cylindrical geometry with the notation commonly used:

$$D_f\left(\frac{d^2\phi_f}{dr^2}+\frac{1}{r}\frac{d\phi_f}{dr}\right) - (\Sigma_s+\Sigma_{af})\phi_f + \nu\Sigma_{ft}\epsilon\,\phi_t = 0$$

$$D_t\left(\frac{d^2\phi_t}{dr^2}+\frac{1}{r}\frac{d\phi_t}{dr}\right) - \Sigma_{at}\,\phi_t + \Sigma_s\phi_f = 0 \quad .$$

$$0 \leq r \leq R \qquad (1)$$

The diffusion coefficient of the thermal-neutron group is neglected in the modified one-group model. This is permissible, because the slowing down area of neutrons is about ten times as great as the diffusion area in a BWR. With this approximation, Eq. (1) is reduced to the simpler form,

$$\tau\left(\frac{d^2\phi_f}{dr^2}+\frac{1}{r}\frac{d\phi_f}{dr}\right) + (k_\infty - 1)\,\phi_f = 0 \quad ,$$

$$0 \leq r \leq R \qquad (2)$$

where τ is the slowing down area (or Fermi age) and k_∞ is the infinite neutron multiplication factor defined by $\tau = \frac{D_f}{\Sigma_s+\Sigma_{af}}$ and $k_\infty = \frac{\nu\Sigma_{ft}\Sigma_s\epsilon}{\Sigma_{at}(\Sigma_s+\Sigma_{af})}$, respectively. Replacing τ by M^2 (the migration area) in order to account for the neutron diffusion effect in the thermal-energy group, the following equation for the fast flux is obtained:

$$M^2\left(\frac{d^2\phi_f}{dr^2}+\frac{1}{r}\frac{d\phi_f}{dr}\right) + (k_\infty - 1)\phi_f = 0 \quad .$$

$$0 \leq r \leq R \qquad (3)$$

Changing the scale of the coordinate such that $r = 1$ at the surface of the reactor R, and using the nondimensional material buckling σ defined by $\sigma = \frac{k_\infty - 1}{M^2}R^2$, Eq. (3) is further reduced to

$$\frac{d^2\phi_f}{dr^2}+\frac{1}{r}\frac{d\phi_f}{dr}+\sigma\phi_f = 0 \qquad 0 \leq r \leq 1 \quad . \qquad (4)$$

The value of σ is averaged over each region by assumptions 1 and 3. Thus, replacing ϕ_f and ϕ, the following final equations are obtained.

$$\frac{d^2\phi}{dr^2} + \frac{1}{r}\frac{d\phi}{dr} + \sigma_1\phi = 0 \qquad 0 \leq r \leq r_1 \qquad \text{inner region}$$

$$\frac{d^2\phi}{dr^2} + \frac{1}{r}\frac{d\phi}{dr} + \sigma_2\phi = 0 \qquad r_1 \leq r \leq r_2 \qquad \text{outer region}$$

$$\frac{d^2\phi}{dr^2} + \frac{1}{r}\frac{d\phi}{dr} - \kappa\phi = 0 \qquad r_2 \leq r \leq 1 \qquad \text{reflector} \ . \tag{5}$$

The solution of Eq. (5) can easily be obtained analytically.

For the reactor to be critical, the following criticality relation is required:

$$\begin{aligned}
&\sqrt{\kappa}\,[AJ_0(\sqrt{\sigma_2}\,r_2) - BY_0(\sqrt{\sigma_2}\,r_2)] \\
&\times [K_0(\sqrt{\kappa})\,I_1(\sqrt{\kappa}\,r_2) - I_0(\sqrt{\kappa})\,K_1(\sqrt{\kappa}\,r_2)] \\
&+ \sqrt{\sigma_2}\,[AJ_1(\sqrt{\sigma_2}\,r_2) - BY_1(\sqrt{\sigma_2}\,r_2)] \\
&\times [K_0(\sqrt{\kappa})\,I_0(\sqrt{\kappa}\,r_2) + I_0(\sqrt{\kappa})\,K_0(\sqrt{\kappa}\,r_2)] = 0 \ ,
\end{aligned} \tag{6}$$

where

$$A = \begin{cases} \sqrt{\sigma_2}\,J_0(\sqrt{\sigma_1}r_1)\,Y_1(\sqrt{\sigma_2}r_1) - \sqrt{\sigma_1}\,J_1(\sqrt{\sigma_1}r_1)\,Y_0(\sqrt{\sigma_2}r_1) & \sigma_1 > 0 \\ \sqrt{\sigma_2}\,Y_1(\sqrt{\sigma_2}r_1) & \sigma_1 = 0 \\ \sqrt{\sigma_2}I_0(\sqrt{\sigma_1}r_1)\,Y_1(\sqrt{\sigma_2}r_1) + \sqrt{\sigma_1}\,I_1(\sqrt{\sigma_1}r_1)\,Y_0(\sqrt{\sigma_2}r_1) & \sigma_1 < 0 \end{cases}$$

$$B = \begin{cases} \sqrt{\sigma_2}\,J_0(\sqrt{\sigma_1}r_1)J_1(\sqrt{\sigma_2}r_1) - \sqrt{\sigma_1}\,J_1(\sqrt{\sigma_1}r_1)\,J_0(\sqrt{\sigma_2}r_1) & \sigma_1 > 0 \\ \sqrt{\sigma_2}\,J_1(\sqrt{\sigma_2}r_1) & \sigma_1 = 0 \\ \sqrt{\sigma_2}I_0(\sqrt{\sigma_1}r_1)J_1(\sqrt{\sigma_2}r_1) + \sqrt{\sigma_1}\,I_1(\sqrt{\sigma_1}r_1)J_0(\sqrt{\sigma_2}r_1) & \sigma_1 < 0 \ . \end{cases}$$

It is assumed that the material buckling of the outer region σ_2 is positive for the practical range of the power distribution.

The effect of the reactivity feedback and of the control rods can be approximately incorporated in Eq. (5) by separating the value of σ_k into each component as

$$\sigma_k = \sigma_{\text{fuel}\,k} - \Delta\sigma_{D_k} - \Delta\sigma_{X_k} - u_k \qquad k = 1, 2 \ , \tag{7}$$

where $\sigma_{\text{fuel}\,k}$ is the nondimensional material buckling of the fuel, which is a function of fuel burnup e; $\Delta\sigma_{D_k}$ and $\Delta\sigma_{X_k}$ are feedback reactivities of Doppler and xenon and u_k is the reactivity suppressed by control rods.

The power density P can be expressed in terms of the fast flux ϕ_f as

$$P = \epsilon\,\Sigma_{ft}\phi_t = \frac{\epsilon\,\Sigma_{ft}}{\Sigma_{at}}\,\Sigma_s\phi_f \ . \tag{8}$$

Noting that $\epsilon\,\Sigma_{ft}/(\Sigma_{at})$ can be replaced by k_∞/ν in one-group theory and using assumption 2, the power density is found to be proportional to the product of the infinite multiplication factor k_∞ and the fast flux ϕ_f. Further, using the relation $k_\infty = 1 + M^2B^2$ between the material buckling $B^2 = \sigma/R^2$ and the infinite multiplication factor k_∞, Eq. (8) can be approximated as

$$P = c(1 + M^2B^2)\phi \ , \tag{9}$$

where c is a normalization coefficient. The reactor power is normalized in this study such that the average power density is unity

$$\int_{\text{core}} P\,dv / V_{\text{core}} = 1 \ . \tag{10}$$

Therefore, the average power density of each region is written as

$$\begin{aligned}
P_1 &= \frac{1}{v_1 + g_0 v_2} \\
P_2 &= g_0 P_1 \ ,
\end{aligned} \tag{11}$$

where

$$g_0 = \frac{1 + M^2B_2^2}{1 + M^2B_1^2}\,g \ , \qquad g = \frac{\phi_2}{\phi_1} \ ;$$

ϕ_k is the average neutron flux in each region and v_k is the volume fraction of each region ($v_1 + v_2 = 1$).

Now the feedback reactivities due to the Doppler effect and to xenon are explicitly expressed using Eq. (11) as

$$\begin{aligned}
\Delta\sigma_{D_k} &= \beta P_k \\
\Delta\sigma_{X_k} &= \frac{\delta(1 + \gamma)}{\gamma + P_k}\,P_k \ ,
\end{aligned} \tag{12}$$

where β, δ, and γ are some given constants and their meanings are self-evident.

The net value σ_k of each region must satisfy the criticality relation in Eq. (6). This relation gives a "zero-power critical curve" in the two-dimensional burnup space with σ_1 and σ_2 as its coordinates. The concept of the burnup space is given in Ref. 13.

The value of ϕ_k, and consequently P_k, is defined at each point on the critical curve. Therefore, the vector $\boldsymbol{\Delta\sigma}_D$ and $\boldsymbol{\Delta\sigma}_X$ can be constructed on this curve and the new critical curve is defined, which can be called the "high-power critical curve". This relation is shown in Fig. 1. If the

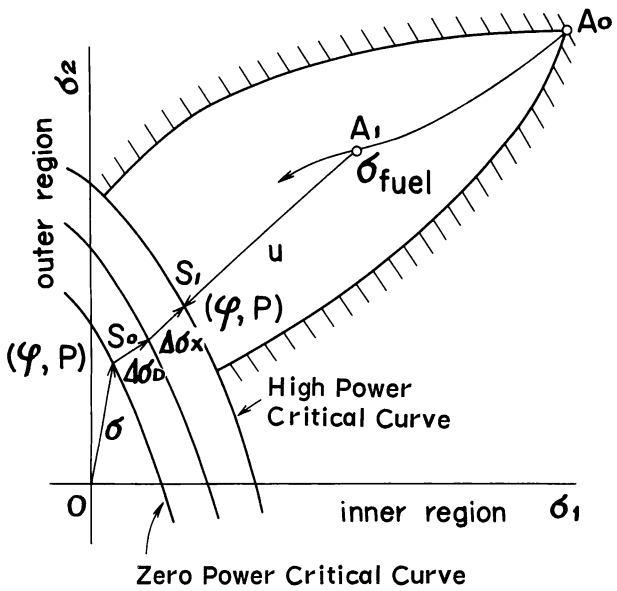

$$\Delta\sigma_D = \beta P \quad \text{(Doppler)}$$

$$\Delta\sigma_x = \frac{\delta(1+\gamma)}{\gamma + P} P \quad \text{(xenon)}$$

Fig. 1. Treatment of feedback reactivities in burnup space.

fuel, originally at A_0, has been depleted to the state A_1, the reactor can be made critical by the proper insertion of the control rods which brings the state A_1 to S_1 somewhere on the high-power critical curve. The net σ is brought to S_0 on the zero-power critical curve by the feedback reactivities calculated by the power at S_1, which is also equal to the power at S_0. Using this power shape, the next gradient of the trajectory is determined. This procedure is continued until the fuel characteristic reaches the high-power critical curve.

Maximum flux ψ_k in each region is also determined by specifying a point on the zero-power critical curve or a corresponding point on the high-power critical curve. Therefore, the power-peaking factor f is also determined at any point on the high-power critical curve

$$f = \frac{\max_k [\psi_k(1 + B_k^2 M^2)]}{\sum_{k=1}^{2} \phi_k(1 + B_k^2 M^2) v_k} . \tag{13}$$

It is noted that the average power density as well as the average neutron flux is determined regardless of the burnup history of the fuels in this model. This is, of course, an approximation.

The two-region reactor model is pictured in Fig. 2, and the characteristics of the reactor are given in Table I.

It is time consuming to perform criticality calculations for the control rod optimization at every instant. Therefore, the main quantities characterizing the critical reactor state are calculated in advance and fitted to each other by the quadratic functions. Neutron flux is used rather than reactor power in the burnup equation. The reason is explained in Sec. IV. The average neutron flux ϕ_k consistent with the power P_k satisfying the constraint of Eq. (10) is given as

$$\phi_1 = \frac{1}{v_1(1 + B_1^2 M^2) + v_2 g(1 + B_2^2 M^2)}$$

$$\phi_2 = g\,\phi_1 . \tag{14}$$

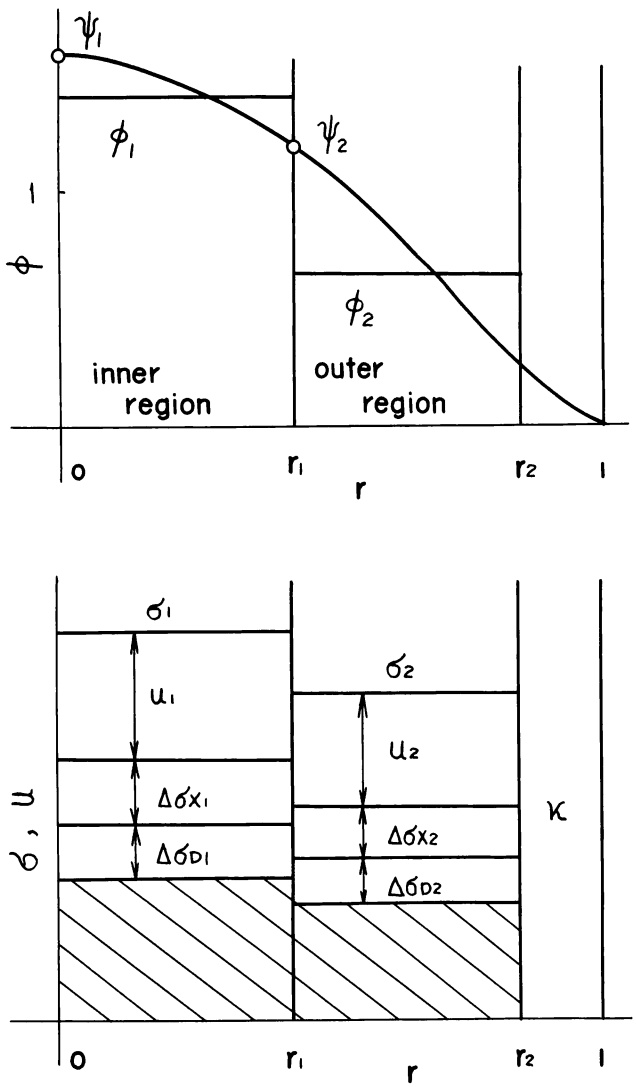

Fig. 2. Two-region reactor model.

TABLE I

Characteristics of a Typical Reactor

Thermal power	P_{th}	1650 MW
Fuel inventory	W	88 ton
Load factor	L_1	0.85
Down time	A	20 days/year
Core radius	R_c	165 cm
Core height	H	365 cm
Reflector thickness	d	12 cm
Migration area	M^2	80 cm^2
Constants for the feedback reactivities		
Doppler	β	2.42
Xenon	γ	0.70
	δ	7.51
Maximum allowable radial power-peaking factor	f	1.40

The constant c in Eq. (9) is set at 1.0. The following five equations are fitted by the least-squares method on the high power critical curve:

$$\sigma_2(\sigma_1) = \sum_{i=0}^{2} A_i \sigma_1^i$$

$$g(\sigma_1) = \sum_{i=0}^{2} B_i \sigma_1^i$$

$$\phi_1(\sigma_1) = \sum_{i=0}^{2} C_i \sigma_1^i$$

$$f(g) = \sum_{i=0}^{3} D_i g^i$$

$$\sigma_1(g) = \sum_{i=0}^{2} E_i g^i \ . \qquad (15)$$

These coefficients must be determined for each value of the volume fraction $v_1(0.2 \rightarrow 0.8)$ determined by the refueling scheme. The relative error introduced in these fittings is within 2% for $f \leq 1.5$, which is thought satisfactory for the present purpose.

III. REFUELING SCHEMES

In general, a line of region numbers can represent the history of the fuel assembly irradiation. For example, 2 1 1 1 1 means that this assembly spends the first refueling interval in the outer region, the next four succeeding intervals in the inner region, and is then discharged. In equilibrium, each assembly follows this rule: one-fourth of the assemblies are removed from the inner region, a corresponding number are moved from the outer region to replace them, and new ones fill the outer region. It is also possible for some assemblies of another line to be in the core at the same time. In general, a description like

2 1 1 1 1 ... 20 assemblies per refueling ... 100 assemblies in the core
1 1 2 ... 40 assemblies per refueling ... 120 assemblies in the core
} total 220 assemblies

can completely specify a refueling scheme.

It can be seen that even for a two-region reactor more than several thousand different schemes exist. It is obvious that a too complicated scheme is not desirable and generally is no more satisfactory; therefore, refueling schemes of a maximum of two lines are used in this paper. Such history as 1 1 2 1 2 calls for many replacements within the core other than loading and discharging and usually has a relatively large local power peaking factor. Thus, only those refueling schemes with one or two lines are selected. Examples are:

one line 1 1 1 2 2 2

one line 2 2 2 1 1 1

two lines 1 1 1, 2 2 2

two lines 1 1 1 2, 2 2 1 1 or 1 1 1 1, 1 2 2 2 etc.

The last one may more nearly represent the actual refueling practice but is rather complicated and is omitted. Only the following three refueling schemes are considered:

1. $J = 0$ Parallel
   (1 1 1, 2 2 $N_1 = 3$, $N_2 = 2$, for example)
2. $J = 1$ Series out-in
   (2 1 1 1 $N_1 = 3$, $N_2 = 1$, for example)
3. $J = -1$ Series in-out
   (1 1 2 2 $N_1 = 2$, $N_2 = 2$, for example).

Refueled or replaced assemblies are scattered and shuffled in each region. The refueling fractions are $1/N_1$ and $1/N_2$, the inverse of the batch numbers (integers) in each region. When $N_1 = N_2 = 1$, the series method reduces to the well-known zone shuffling. For fuel assemblies to be transferred neither more nor less for series schemes, the batch numbers and the volume fractions must satisfy these relations: $v_1 = N_1/(N_1 + N_2)$ and $v_2 = N_2/(N_1 + N_2)$, whereas no such relations are necessary for parallel schemes.

We distinguish these parallel refueling schemes in which the batch number of each region is the same ($N_1 = N_2$) and the volume fraction v_1 is different. The difference in v_1 defines the difference in the range of the fuel shuffling within the region, which is necessary to reduce the local power peaking caused by the spatial irregularity in fuel burnup. Schematic diagrams of these three refueling schemes are shown in Fig. 3.

The refueling interval T is determined in an equilibrium cycle by the following five quantities:

1. average burnup of the discharged fuels $\bar{e}$
2. average refueling fraction of the core D
3. specific power S_p
4. load factor L_1
5. availability L_2.

$$T = \frac{\bar{e}D}{S_p L_1 L_2} \quad , \tag{16}$$

where

$$\bar{e} = \begin{cases} \dfrac{e_1 \dfrac{v_1}{N_1} + e_2 \dfrac{v_2}{N_2}}{\dfrac{v_1}{N_1} + \dfrac{v_2}{N_2}} & \text{parallel} \\ e_1 & \text{out-in} \\ e_2 & \text{in-out} \end{cases}$$

$$D = \begin{cases} \dfrac{v_1}{N_1} + \dfrac{v_2}{N_2} & \text{parallel} \\ \dfrac{1}{N_1 + N_2} & \text{series} \end{cases}$$

$$S_p = \frac{P_{th}}{W}$$

$$L_1 = \frac{\text{actual power}}{\text{rated power}}$$

and

$$L_2 = \frac{\text{operation period}}{\text{refueling interval}}$$

$$= \frac{\bar{e}D}{\bar{e}D + A S_p L_1} \quad . \tag{17}$$

The discharge burnup of each region is denoted as e_1, e_2 and the meaning of the other notations is given in Table I.

It is the current operational requirement that the refueling interval must be one year, which comes from the necessity for reactor maintenance, and the refueling is carried out during this downtime. Using the values in Table I, this condition requires that

J	Scheme		Parameters
0	Parallel		N_1, N_2, v_1
1	Series	Out-in	N_1, N_2, $v_1 = \frac{N_1}{N_1 + N_2}$
-1		In-out	

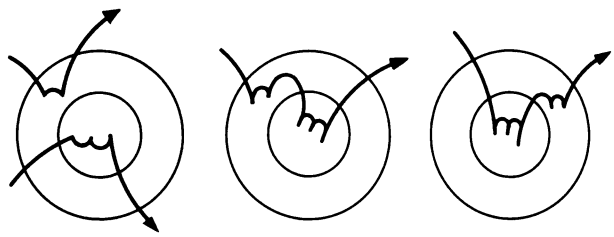

N_1, N_2 Batch Number; inverse Refueling Fraction

v_1 Volume Fraction of the inner Region

Fig. 3. Variety of refueling schemes considered.

$$\bar{e}D = 5500 \text{ MWd/T} \quad . \tag{18}$$

This means that the average fuel burnup increment in one year is required to be constant. Therefore, the object of the control rod programming optimization should be to minimize the required enrichment of feed fuels rather than to maximize the average burnup of discharge fuels. These two optimization problems, however, are shown to be equivalent in Sec. VI. There are many refueling schemes even if the type of the refueling is restricted to the three mentioned above. We restrict the value of D to 0.25 and 0.2, and thus the corresponding discharge burnups become 22000 MWd/T and 27500 MWd/T, respectively. Thirty refueling schemes satisfying this condition are considered. These are listed in Table II.

IV. BURNUP CHARACTERISTICS AND EQUILIBRIUM CONDITIONS

There exist N_k groups of fuels in each region which have different burnup histories and thus different nuclear characteristics. However, all of them can be thought to be exposed in an approximately common flux field in each region. Therefore, the neutron-flux time increment in one refueling interval is thought to be common for all

TABLE II

Proposed Refueling Schemes Satisfying the Condition of One-Year Refueling Interval

$\bar{e}$ = 22000 MWd/T, D = 0.25					$\bar{e}$ = 27500 MWd/T, D = 0.20				
No.	J	N_1	N_2	v_1	No.	J	N_1	N_2	v_1
1	0	6	3	1/2	16	0	6	4	3/5
2	0	6	2	3/4	17	0	6	3	4/5
3	0	5	3	5/8	18	0	5	5	1/3
4	0	4	4	1/3	19	0	5	5	1/2
5	0	4	4	1/2	20	0	5	5	2/3
6	0	4	4	2/3	21	0	4	6	2/5
7	0	3	6	1/2	22	0	3	6	1/5
8	0	3	5	3/8	23	1	4	1	4/5
9	0	2	6	1/4	24	1	3	2	3/5
10	1	3	1	3/4	25	1	2	3	2/5
11	1	2	2	2/4	26	1	1	4	1/5
12	1	1	3	1/4	27	-1	4	1	4/5
13	-1	3	1	3/4	28	-1	3	2	3/5
14	-1	2	2	2/4	29	-1	2	3	2/5
15	-1	1	3	1/4	30	-1	1	4	1/5

the assemblies in each region, although the burnup increment is not. It is, therefore, convenient to use neutron-flux time θ rather than fuel burnup e to express the fuel characteristics.

The fuel characteristics σ and the fuel burnup e can be approximated by the polynominals of the fast neutron-flux time θ.

$$\sigma = \sum_{n=0}^{N_0} a_n \theta^n$$

$$e = \sum_{m=1}^{M_0} b_m \theta^m \quad . \tag{19}$$

These equations are dependent on each other. In fact, the second equation can be derived from the first by integrating Eq. (20), obtained from Eq. (9), and, consequently, $M_0 = N_0 + 1$

$$\frac{de}{d\theta} = c\left(1 + \frac{M^2}{R^2}\sum_{n=0}^{N_0} a_n \theta^n\right) \quad . \tag{20}$$

It was assumed, however, that the above relation has been obtained independently by a more detailed burnup calculation, in which case there is no relation between N_0 and M_0.

Let Θ_k be the flux time increment during one refueling interval, θ_k the flux time accumulated from the latest refueling in each region ($k = 1, 2$), and $\delta_{i,j}$ Kronecker's delta. The flux time of the i'th group of fuels in the k'th region (θ_k^i) can be expressed as

$$\theta_k^i = (i - 1)\,\Theta_k + \tilde{\Theta} + \theta_k$$

$$\tilde{\Theta} = \delta_{J,1}\delta_{k,1} N_2 \Theta_2 + \delta_{J,-1}\delta_{k,2} N_1 \Theta_1 \quad . \tag{21}$$

The nuclear characteristic σ_k, averaged over each region, is obtained by the following operation

$$\sigma_k = \sum_{i=1}^{N_k} \sigma(\theta_k^i)/N_k = \sum_{i=1}^{N_k}\sum_{n=0}^{N_0} a_n[(i - 1)\Theta_k + \tilde{\Theta} + \theta_k]^n/N_k \quad . \tag{22}$$

Therefore, the burnup equation, i.e., the system equation, is given by differentiating Eq. (22)

$$\dot{\sigma}_k = \sum_{i=1}^{N_k}\sum_{n=1}^{N_0} n\, a_n[(i - 1)\Theta_k + \tilde{\Theta} + \theta_k]^{n-1}\phi_k/N_k$$

$$\dot{\theta}_k = \phi_k \qquad k = 1, 2 \quad . \tag{23}$$

The initial and final conditions are

$$\theta_{ki} = 0 \quad , \quad \theta_{kf} = \Theta_k$$

$$\sigma_{ki} = \sum_{i=1}^{N_k}\sum_{n=0}^{N_0} a_n[(i - 1)\Theta_k + \tilde{\Theta}]^n/N_k$$

$$\sigma_{kf} = \sum_{i=1}^{N_k}\sum_{n=0}^{N_0} a_n(i\Theta_k + \tilde{\Theta})^n/N_k \quad . \tag{24}$$

Using the first of Eq. (17), the discharge burnup is given by

$$\bar{e} = \frac{N_1 N_2}{N_1 v_2 + N_2 v_1}\left[\frac{v_1}{N_1}\sum_{m=1}^{M_0} b_m (N_1\Theta_1)^m + \frac{v_2}{N_2}\sum_{m=1}^{M_0} b_m (N_2\Theta_2)^m\right] \quad \text{parallel}$$

$$\bar{e} = \sum_{m=1}^{M_0} b_m (N_1\Theta_1 + N_2\Theta_2)^m \quad \text{series} \quad . \tag{25}$$

Note that the discharge burnups expressed in terms of the flux time are the same for out-in and in-out schemes.

It is evidently disadvantageous to terminate the the operation while some of the control rods are still in the core, except for the situations in which it becomes impossible to continue the operation without violating the constraint on the power peaking. Therefore, the trajectories must terminate on the target curve shown in Fig. 4. At points B and C the power-peaking factors are equal to the design limit. The flux time increments Θ_k can be obtained at any point on the target curve by the last of Eqs. (24); with this Θ_k, the initial states

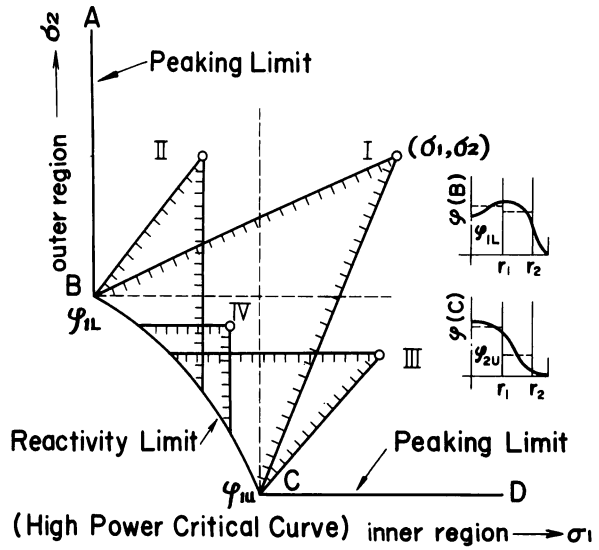

Fig. 4. Target curve on which the trajectories must terminate, and the range of the admissible control.

σ_{ki} and the discharge burnup $\bar{e}$ are uniquely determined by the second part of Eqs. (24) and (25)

$$\sigma_{kf} \rightarrow \Theta_k \begin{cases} \rightarrow \sigma_{ki} \\ \rightarrow \bar{e} \end{cases} .$$

The reactor must be made critical by the non-negative elements of control rods u_k that can bring the reactor state somewhere on the target curve BC. The average flux in the inner region ϕ_1 increases monotonically along the curve from $B(\phi_{1L})$ to $C(\phi_{1U})$. Therefore, the range of the admissible control u_k can be expressed in terms of the admissible range of ϕ_1. This range can be written using Eq. (15) separately for the four cases, depending on the situation of the fuel characteristics (σ_1, σ_2), as shown in Fig. 4.

$$\begin{aligned} &\phi_{1L} \leqslant \phi_1 \leqslant \phi_{1U} && \text{Region I} \\ &\phi_{1L} \leqslant \phi_1 \leqslant \phi_1(\sigma_1) && \text{Region II} \\ &\phi_1[\sigma_1^{-1}(\sigma_2)] \leqslant \phi_1 \leqslant \phi_{1U} && \text{Region III} \\ &\phi_1[\sigma_1^{-1}(\sigma_2)] \leqslant \phi_1 \leqslant \phi_1(\sigma_1) && \text{Region IV} \quad . \end{aligned} \tag{26}$$

This range generally can be written as

$$G(\sigma_1, \sigma_2, \phi_1) \geqslant 0 \quad . \tag{27}$$

The average flux in the outer region ϕ_2 can be determined by ϕ_1; i.e., $\phi_2 = g(\phi_1) \cdot \phi_1$.

The problem is now completely defined: to maximize the discharge burnup of Eq. (25) while satisfying Eq. (23), the boundary conditions of Eq. (24) and the constraint of Eq. (26).

Burnup characteristics of a typical BWR (Table I) were calculated by the three-group point burnup code for the two kinds of fuels with different enrichments. The void fraction was set at 30%. The results are shown in Fig. 5. These relations can be well fitted by the quadratic functions. However, the actual calculations were performed by approximating these relations to be linear to facilitate manipulation of the equations. This treatment will introduce the quantitative error in the calculated burnup or enrichment, but will not affect the nature of the optimal policy of control rod programming. The effect of the enrichment is also taken in linear form

$$\begin{aligned} &\sigma = a\theta + \sigma_0 \quad , \qquad \sigma_0 = \gamma\eta + \delta \\ &\theta = (\alpha\eta + \beta)e \quad . \end{aligned} \tag{28}$$

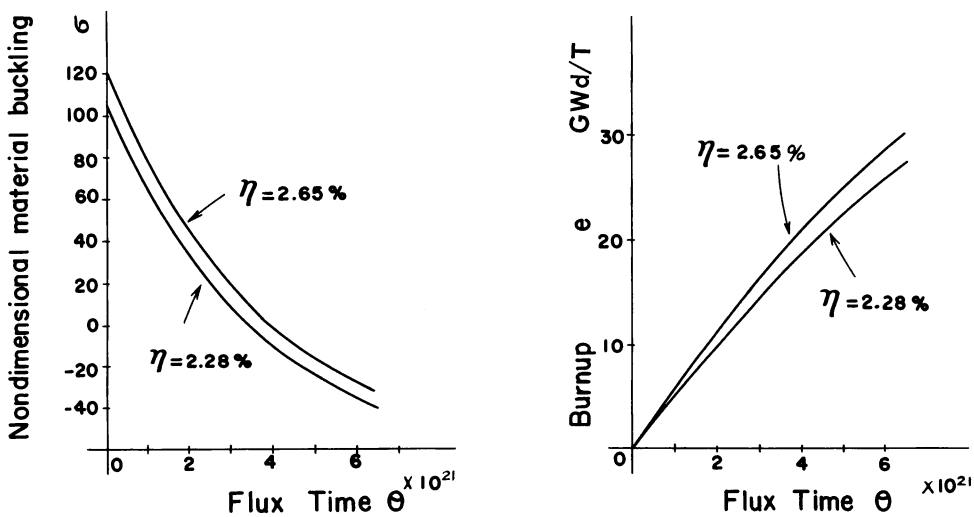

Fig. 5. Burnup characteristics of fuel assemblies (void fraction = 30%).

The value of the neutron flux ϕ_k, calculated from Eq. (14), is not consistent with the actual power used in the calculation of Fig. 5. This can be accommodated by suitably choosing the depletion coefficient a, but this selection only serves to change the time scale and does not affect the trajectory itself. It is sufficient to specify the relation between σ and e (MWd/T)

$$\sigma = a(\alpha\eta + \beta)e + \gamma\eta + \delta \quad . \tag{29}$$

The coefficients are

$$a\alpha = -0.000147 \quad , \qquad a\beta = -0.00535$$

$$\gamma = 46.0 \quad , \qquad \delta = -1.8 \quad .$$

Using Eqs. (28) and (29), the following equations characterizing the system are obtained corresponding to Eqs. (23) through (25)

$$\dot{\sigma}_k = a\phi_k \tag{30}$$

$$\sigma_{ki} = a\left(\frac{N_k - 1}{2}\Theta_k + \tilde{\Theta}\right) + \sigma_0$$

$$\sigma_{kf} = a\left(\frac{N_k + 1}{2}\Theta_k + \tilde{\Theta}\right) + \sigma_0 \tag{31}$$

$$\Theta_k = \frac{2}{a(N_k + 1)}\left[\sigma_{kf} - \delta_{J,1}\delta_{k,1}\Theta_2^0 + \delta_{J,-1}\delta_{k,2}\Theta_1^0 - (\delta_{J,1}\delta_{k,2} + \delta_{J,-1}\delta_{k,1} + \delta_{J,0})\sigma_0\right]$$

$$\Theta_k^0 = -\frac{2N_k}{N_k + 1}\sigma_{kf} + \frac{N_k - 1}{N_k + 1}\sigma_0 \tag{32}$$

$$\bar{e} = \frac{2N_1N_2}{a(N_1v_2 + N_2v_1)(\alpha\eta + \beta)}\left[\frac{v_1}{N_1 + 1}(\sigma_{1f} - \sigma_0) + \frac{v_2}{N_2 + 1}(\sigma_{2f} - \sigma_0)\right] \quad \text{parallel}$$

$$\bar{e} = \frac{2}{a(N_1 + 1)(\alpha\eta + \beta)}\left[N_1\sigma_{1f} - \frac{N_2(N_1 - 1)}{N_2 + 1}\sigma_{2f} - \frac{N_1 + N_2}{N_2 + 1}\sigma_0\right] \quad \text{out-in}$$

$$\bar{e} = \frac{2}{a(N_2 + 1)(\alpha\eta + \beta)}\left[N_2\sigma_{2f} - \frac{N_1(N_2 - 1)}{N_1 + 1}\sigma_{1f} - \frac{N_1 + N_2}{N_1 + 1}\sigma_0\right] \quad \text{in-out} \quad . \tag{33}$$

V. OPTIMAL TERMINAL STATE AND OPTIMAL CONTROL ROD PROGRAMMING

The optimal control rod programming without refueling was obtained in Ref. 13 by using the maximum principle where the optimal trajectories were calculated by the time-reversal analysis such that the inverse time trajectory passed through the initial state. The results obtained correspond to the special case of the parallel refueling schemes with $N_1 = N_2 = 1$. For reference, the optimal trajectories from various initial states are shown in Fig. 6. Optimal policy depends on the position of the initial state. The initial state must be within the region *GBCF* to be able to terminate the operation with all the rods withdrawn. The state *C* on the critical curve gives the minimum total buckling where the burnup is maximum. Therefore, it is best to try to arrive at this point as nearly as possible. Initial states within the region *EHCF* can reach the optimal terminal state *C* and the optimal trajectory is not unique and degenerate except for those on the trajectories *EHC* and *FC*. We call this policy the degenerate policy. The power density of the outer region should be as high as possible for these initial states within the region *ABCHE*. Let the power distribution at the state *B* and *C* be denoted as maximum allowable outer high distribution (MAOHD) and maximum allowable inner high distribution (MAIHD). The power distribution is MAOHD throughout the reactor life for the initial states within the region *ABG*. However, for the initial states within the region *GBCHE*, the power distribution is MAOHD until the trajectory reaches the line *BH* where the outer rods are completely withdrawn (for the initial states within the region

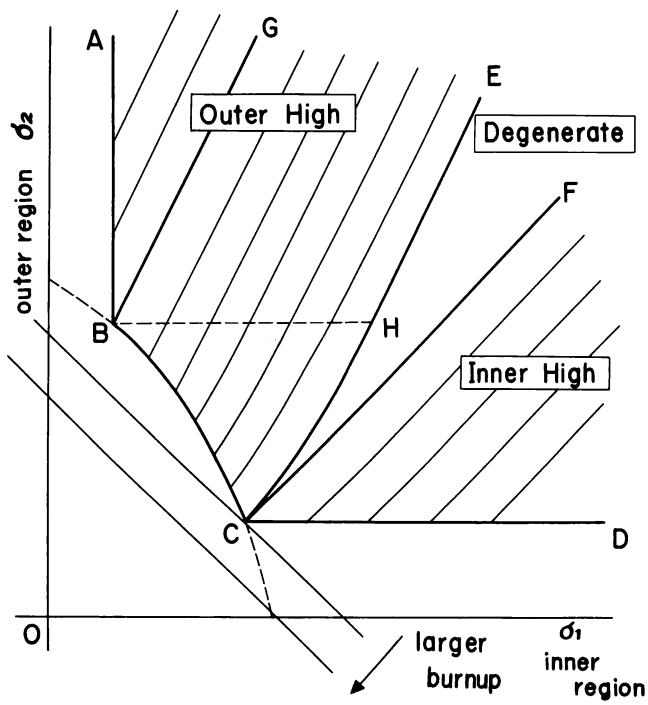

Fig. 6. Synthesis of optimal trajectories (no refueling, $v_1 = 0.5$).

GBHE only), and then the power peak is gradually shifted into the inner region, the reactor being critical with only the inner rods inserted. We call these policies outer high policy. For these initial states within the region *FCD*, the power density of the inner region should be as high as possible and its distribution is MAIHD through the reactor life. We call this policy inner high policy.

A characteristic of the present problem with refueling is that the initial state, which is the average of the N_k groups of fuels, is not given although the nuclear characteristic of the new fuel σ_0 is. This state can be expressed in terms of the average final state which must be somewhere on the target curve

$$\sigma_{1i} = \frac{N_1 - 1}{N_1 + 1}\sigma_{1f} + \frac{2}{N_1 + 1}\sigma_0$$

$$\sigma_{2i} = \frac{N_2 - 1}{N_2 + 1}\sigma_{2f} + \frac{2}{N_2 + 1}\sigma_0 \qquad \text{parallel}$$

$$\sigma_{1i} = \frac{N_1 - 1}{N_1 + 1}\sigma_{1f} + \frac{4N_2}{(N_1 + 1)(N_2 + 1)}\sigma_{2f} - \frac{2(N_2 - 1)}{(N_1 + 1)(N_2 + 1)}\sigma_0$$

$$\sigma_{2i} = \frac{N_2 - 1}{N_2 + 1}\sigma_{2f} + \frac{2}{N_2 + 1}\sigma_0 \qquad \text{out-in}$$

$$\sigma_{1i} = \frac{N_1 - 1}{N_1 + 1}\sigma_{1f} + \frac{2}{N_1 + 1}\sigma_0$$

$$\sigma_{2i} = \frac{4N_1}{(N_1 + 1)(N_2 + 1)}\sigma_{1f} + \frac{N_2 - 1}{N_2 + 1}\sigma_{2f} - \frac{2(N_1 - 1)}{(N_1 + 1)(N_2 + 1)}\sigma_0 \quad . \qquad \text{in-out} \qquad (34)$$

This is illustrated for the simplest case of the out-in zone shuffling ($N_1 = N_2 = 1$) in Fig. 7. The final state of the outer region must be equal to the initial state of the inner region ($\sigma_{2f} = \sigma_{1i}$) and the contour of the discharge burnup is parallel to the σ_2 axis $\left(\bar{e} = \{1/[a(\alpha\eta + \beta)]\}(\sigma_{1f} - \sigma_0)\right)$. The state C is no more an optimal terminal state because the burnup at β is greater than at α. It could be easily shown that the burnup at α is greater than at β for the in-out zone shuffling. Another characteristic of this problem is that the average discharge burnup, expressed in terms of the flux time, is equal for both out-in and in-out schemes, as shown in Eq. (25). Therefore, the formal treatment by the maximum principle cannot distinguish the difference in the optimal controls for the two opposite series schemes. However, this problem can be solved directly knowing that the discharge burnup is uniquely determined at any point on the target curve as shown in Eq. (33). In other words, this is a terminal control problem. The optimal terminal state or the direction in which the average discharge burnup increases is determined

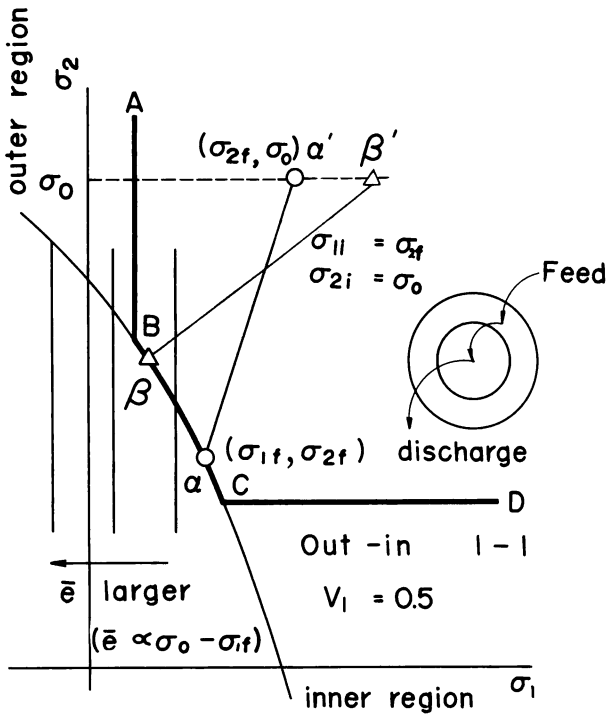

Fig. 7. Initial and final states in equilibrium (out-in zone shuffling).

by Eq. (33). Contours of the discharge burnup are a group of lines with the negative gradient $-v_1(N_2 + 1)/[v_2(N_1 + 1)]$ for the parallel scheme and the positive gradients $N_1(N_2 + 1)/[N_2(N_1 - 1)]$ and $N_1(N_2 - 1)/[N_2(N_1 + 1)]$ for the out-in and in-out schemes, respectively. These lines are shown in Fig. 8. It is evident that the discharge burnup increases monotonically along the target curve from D to A for an out-in scheme and from A to D for an in-out scheme. When $N_1 = N_2 = 1$, the values for the out-in scheme on the line AB are equal to each other; likewise, those for the in-out scheme on the line CD are equal. Therefore, the optimal terminal states for series schemes are the points S_0 at which the values of the nuclear characteristics of the outer region (out-in) and the inner region (in-out) at the final states are equal to that of the new fuel σ_0. It is noted that the control rods should remain in one or the other region at these points. There are three situations in the parallel scheme depending on the values of the refueling parameters N_1, N_2, v_1. Let the point at which the contour of the burnup is tangent to the critical curve be denoted as $E(\sigma_{1T}, \sigma_{2T})$. This point is obtained by Eqs. (15) and (33) as

$$\sigma_{1T} = -\frac{W_1 + W_2 A_2}{2 W_2 A_1}$$

$$\sigma_{2T} = A_1\sigma_{1T}^2 + A_2\sigma_{1T} + A_3 \quad , \qquad (35)$$

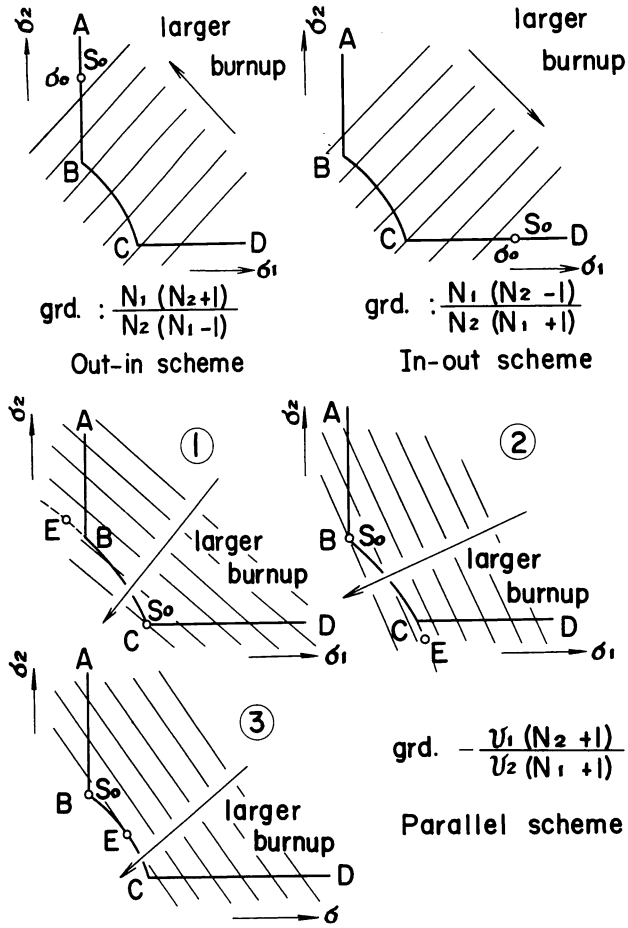

Fig. 8. Contours of the discharge burnup and optimal terminal state.

where

$$W_k = \frac{2v_k}{a(N_k + 1)(\alpha\eta + \beta)} \quad .$$

When the tangent point E is to the left of B, the burnup increases along the target curve from A to C and from D to C, and C is the optimal terminal state (Case 1). When it is to the right of C, the burnup increases along the target curve from A to B and from D to B, and B is the optimal terminal state (Case 2). When it is between B and C, the burnup increases along the target curve from A to B, from E to B, from E to C and from D to C, and either B or C becomes the optimal terminal state (Case 3). Among the candidates in Table II, two (Nos. 9 and 22) belong to Case 2, one (No. 7) to Case 3, and the others to Case 1 for the maximum allowable power-peaking factor $f = 1.4$.

The nature of the optimal terminal state is now clear and the problem is to find the best terminal state σ_f attainable from the initial state σ_i defined by Eq. (31) or Eq. (34). If the optimal terminal state is attainable from its corresponding initial state, this set gives the optimal solution and the control rod programmings that combine these states are usually not unique and are degenerate. This situation will occur only in the parallel scheme, because it is impossible to transfer the state without being at least partly exposed in either region, which is required for the series schemes. If the optimal terminal state is not attainable, the optimal solution can be shown to be on one of the boundary curves by examining the nature of the attainable region and the relation between the initial and the final states.

In Ref. 13 the control rod density u_1 was chosen as the control variable. However, it is convenient to regard the average flux in the inner region ϕ_1 as the control variable because the right side of Eq. (30) does not contain σ and is a function of ϕ_1 only, and the constraint on u_1 can be replaced by the constraint on ϕ_1 as shown in Eq. (26). The set of initial states that can attain the given final state σ_f^j on the target curve is defined as Γ^j. This set covers a certain range in the burnup space and is calculated by the time-reversal analysis. The range of the control variable ϕ_1 monotonically increases starting from one permissible value until the upper and the lower limit become fixed by the constraint on the power-peaking factor. The flux ratio g monotonically decreases toward the lower right of the critical curve. From Eqs. (26) and (30), the gradient of the trajectory can be expressed as

$$g(\sigma_1) \leqslant \frac{d\sigma_2}{d\sigma_1} \leqslant g[\sigma_1^{-1}(\sigma_2)] \equiv g(\sigma_2) \quad . \qquad (36)$$

Integration of Eq. (36) defines the attainable region Γ and the trajectories by the boundary value control $G(\sigma_1, \sigma_2, \phi_1) = 0$ give the two boundary curves. The gradient of the upper boundary curve monotonically increases and that of the lower boundary curve monotonically decreases until they are fixed by the constraint on the power-peaking factor. These attainable regions Γ are illustrated in Fig. 9 for five final states in case of the out-in 3-2 scheme. Any initial state inside the region Γ can attain the final state and the trajectories are not unique. The trajectory is unique only when the initial state is on the boundary curves. An initial state outside the region Γ can not attain the final state by any means. In general, we call the policy of operation along the upper boundary curve as outer high policy and that along the lower boundary curve as inner high policy. The same argument leads to the definition of the attainable region from a given initial state. In this case, the role of the upper and the lower boundary curves should be interchanged. When the final state moves on the target curve, the upper and lower

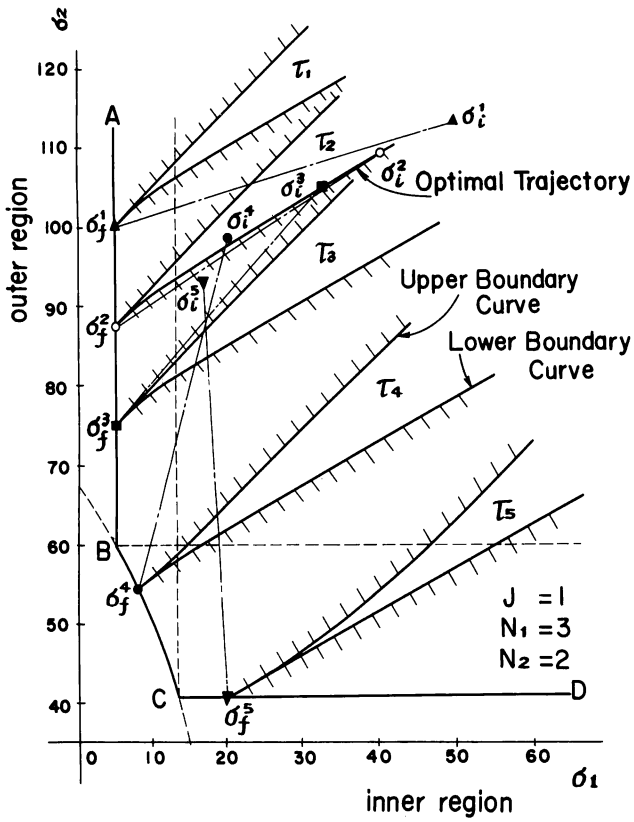

Fig. 9. Attainable region and optimal trajectory (out-in 3-2, η = 2.65%).

boundary curves move in parallel both horizontally and vertically. This is because the maximum gradient of the trajectory is determined only by σ_2 and the minimum gradient only by σ_1, until each becomes a constant determined by the constraint on the power-peaking factor. Therefore, boundary curves (upper or lower) entering into different final states do not intersect each other, and the entire space of the supercritical region is completely covered with these boundary curves.

We can now prove the following facts:

1. The policy of the optimal control rod programming is inner high for the out-in scheme.

2. The policy of the optimal control rod programming is outer high for the in-out scheme.

3. The policy of the optimal control rod programming is either outer high or inner high for the parallel scheme, unless the optimal terminal state is attainable. Otherwise, it is degenerate.

Proof: The nature of the boundary trajectories and that of the variational equations of Eqs. (34) are used.

1. *Out-in scheme*. Assume that a set of the initial state σ_i^0 and the final state σ_f^0 is exactly on some lower boundary curve and that this set is not optimal. This assumption requires that for the state σ_f^0 to become optimal it must move along the target curve so that $\delta\sigma_{1f} \leq 0$ and/or $\delta\sigma_{2f} \geq 0$ hold. The effect of the changes of the final state on the changes of the initial state in equilibrium is given as

$$\delta\sigma_{1i} = \frac{N_1 - 1}{N_1 + 1}\,\delta\sigma_{1f} + \frac{4N_2}{(N_1 + 1)(N_2 + 1)}\,\delta\sigma_{2f}$$

$$\delta\sigma_{2i} = \frac{N_2 - 1}{N_2 + 1}\,\delta\sigma_{2f} \quad . \tag{37}$$

The lower boundary curves are divided into three cases depending on the position of the final state. This is shown in Fig. 10. From Eq. (37) the following relations are obtained:

$\delta\sigma_{1i} > 0$, $0 < \delta\sigma_{2i} < \delta\sigma_{2f}$ Case a

$\delta\sigma_{1f} < \delta\sigma_{1i}$, $\delta\sigma_{1f} < 0$, $0 < \delta\sigma_{2i} < \delta\sigma_{2f}$ Case b

$\delta\sigma_{1f} < \delta\sigma_{1i} < 0$, $\delta\sigma_{2i} = 0$ Case c .

The range of the variations of the initial state is shown as shaded regions of lines with a negative gradient

region $\gamma\alpha\sigma_i^0\delta$ Case a

region $\gamma\alpha\beta\delta$ Case b

region $\alpha\sigma_i^0$ Case c .

It becomes a line for Case c. It is evident for Cases a and c that each region is outside the attainable region Γ by the relation $\overline{\sigma_i^0\alpha} = \overline{\sigma_f^0\sigma_f}$. For Case b, let α be chosen such that $\overline{\sigma_i^0\alpha} = \overline{\sigma_f^0\sigma_f}$ and let ϵ and ϵ' be the states on the lower boundary curve starting from σ_f at which the first coordinates are equal to σ_{i1}^0 and σ_{f1}^0, respectively. Then $\overline{\alpha\epsilon} = \overline{\sigma_f\epsilon'}$ because $\overline{\sigma_i^0\epsilon} = \overline{\sigma_f^0\epsilon'}$. The gradient of the lower boundary curve at ϵ' is greater than at ϵ. Therefore this region is always outside the attainable region Γ.

Thus, any final state σ_f which gives larger burnup is proved to be unattainable from its initial state σ_i. This contradicts the assumption, and σ_f^0 is the optimal final state and the optimal policy is inner high.

2. *In-out scheme*. Only the necessary relations are given below, as the method of the proof is completely the same as for the out-in scheme except that the region numbers are interchanged and the control policy is reversed.

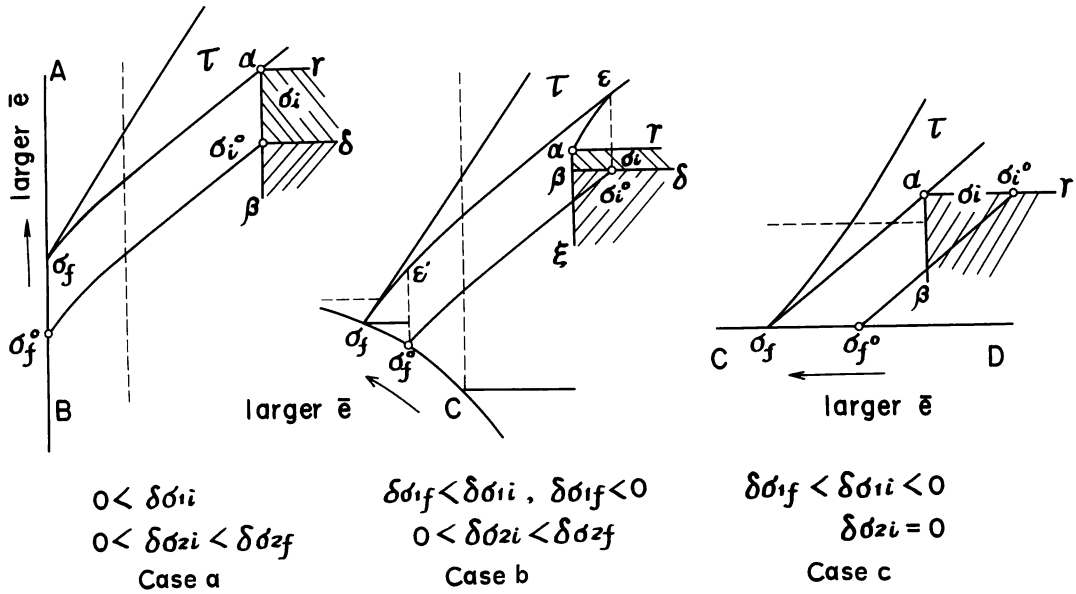

Fig. 10. Explanation of optimal trajectory for out-in scheme.

Variational equation:

$$\delta\sigma_{1i} = \frac{N_1 - 1}{N_1 + 1}\,\delta\sigma_{1f}$$

$$\delta\sigma_{2i} = \frac{4N_1}{(N_1 + 1)(N_2 + 1)}\,\delta\sigma_{1f} + \frac{N_2 - 1}{N_2 + 1}\,\delta\sigma_{2f} \quad . \quad (38)$$

The range of the variations of the initial state:

$\delta\sigma_{1i} = 0$, $\delta\sigma_{2f} < \delta\sigma_{2i} < 0$ Case a

$0 < \delta\sigma_{1i} < \delta\sigma_{1f}$, $\delta\sigma_{2f} < \delta\sigma_{2i}$, $\delta\sigma_{2f} < 0$ Case b

$0 < \delta\sigma_{1i} < \delta\sigma_{1f}$, $0 < \delta\sigma_{2i}$ Case c .

The corresponding region:

region $\sigma_i^0\alpha$ Case a

region $\gamma\alpha\beta\delta$ Case b

region $\gamma\alpha\sigma_i^0\delta$ Case c .

These relations are shown in Fig. 11.

3. *Parallel scheme.* The upper and the lower boundary curves are divided in two cases each depending on the way the burnup increases along the target curve. This is shown in Fig. 12. Only the necessary relations are given below, as the method of the proof is essentially the same as with series schemes.

Variational equation:

$$\delta\sigma_{1i} = \frac{N_1 - 1}{N_1 + 1}\,\delta\sigma_{1f}$$

$$\delta\sigma_{2i} = \frac{N_2 - 1}{N_2 + 1}\,\delta\sigma_{2f} \quad . \quad (39)$$

The range of the variations of the initial state:

$\delta\sigma_{1i} = 0$, $\delta\sigma_{2f} < \delta\sigma_{2i} < 0$ Case a

$\delta\sigma_{1f} < \delta\sigma_{1i} < 0$, $0 < \delta\sigma_{2i} < \delta\sigma_{2f}$ Case b

$0 < \delta\sigma_{1i} < \delta\sigma_{1f}$, $\delta\sigma_{2f} < \delta\sigma_{2i} < 0$ Case c

$\delta\sigma_{1f} < \delta\sigma_{1i} < 0$, $\delta\sigma_{2i} = 0$ Case d .

The corresponding region:

region $\sigma_i^0\alpha$ Cases a and d

region $\gamma\alpha\beta\sigma_i^0$ Cases b and c .

When σ_f^0 is the optimal terminal state and this is attainable, the policy is degenerate except for the special case in which σ_i^0 is on one of the boundary curves.

An example of the optimal trajectories is shown in Fig. 9. With these results, the optimal control rod programming and the corresponding optimal trajectories can be synthesized in the burnup space. These are shown in Figs. 13, 14 and 15. In Fig. 15, Q is the state at which the discharge burnup is equal to that at C (Case 3) and B (Case 4).

The trajectories determined by the conventional constant power shape operation are shown in Fig. 16 as reference. These are obtained by choosing a final state on the critical curve first and then drawing a line in the opposite direction with the gradient corresponding. The control policy of this operation is to make the flux ratio g constant throughout the life of a reactor such that Eq. (40) holds

$$g = \Theta_2/\Theta_1 \quad . \quad (40)$$

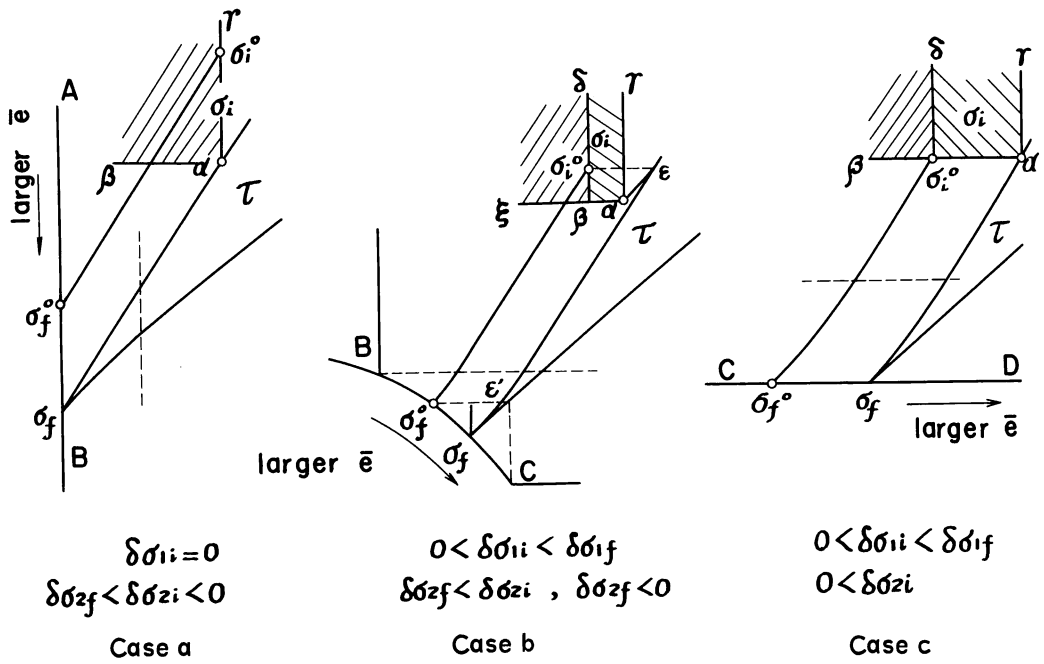

Fig. 11. Explanation of optimal trajectory for in-out scheme.

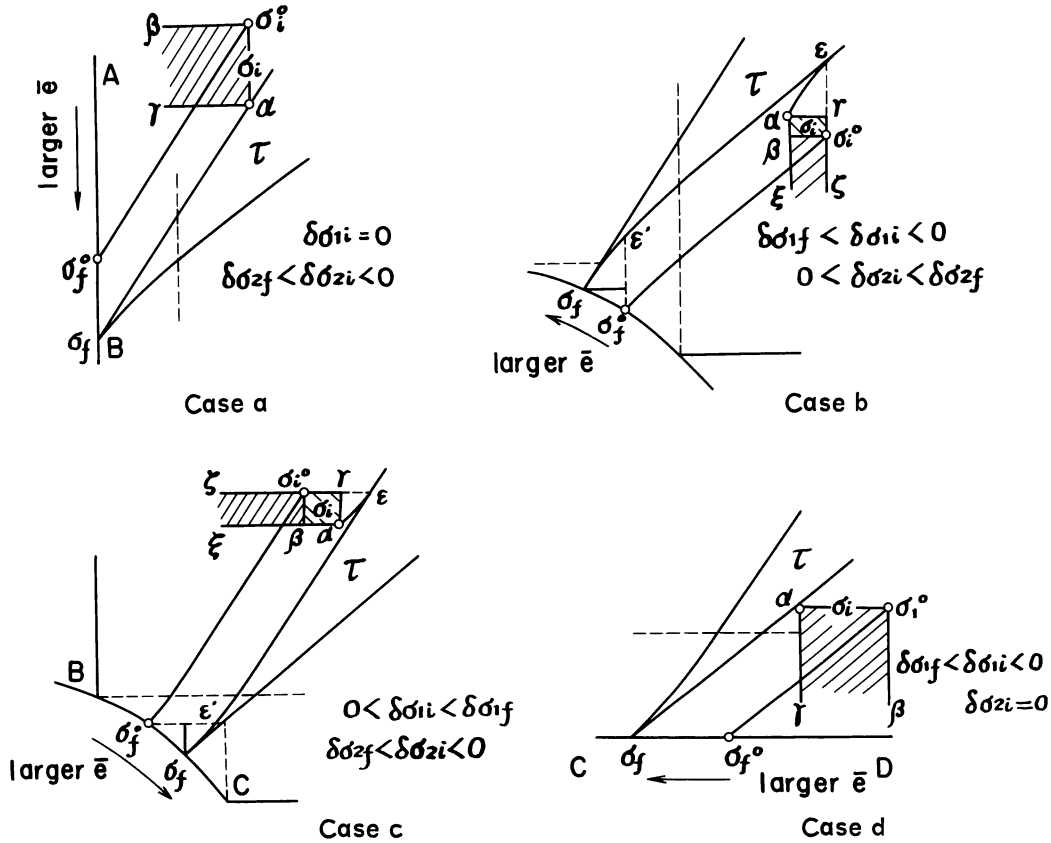

Fig. 12. Explanation of optimal trajectory for parallel scheme.

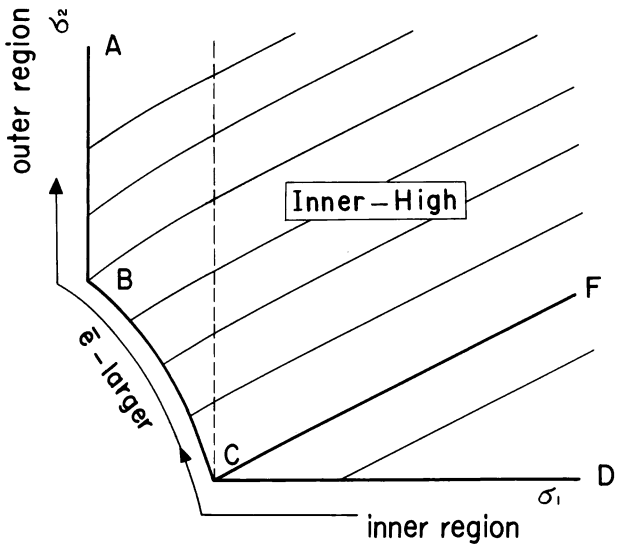

Policy: Power density in the inner region as high as possible

Fig. 13. Synthesis of optimal control for out-in scheme.

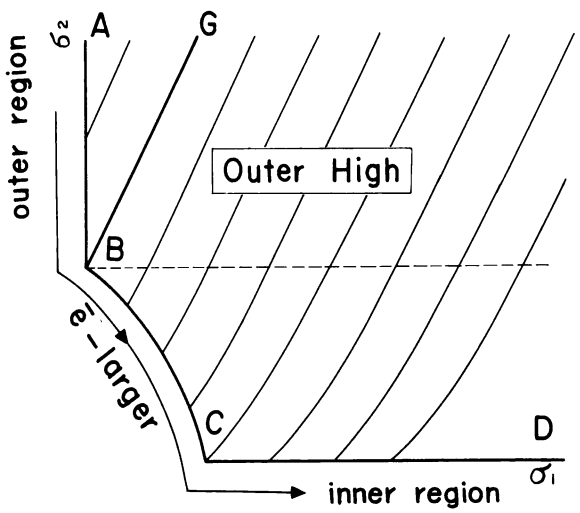

Policy: Power density in the outer region as high as possible

Fig. 14. Synthesis of optimal control for in-out scheme.

VI. EQUIVALENCE OF BURNUP MAXIMIZATION AND ENRICHMENT MINIMIZATION

The problem so far formulated is to maximize the average discharge burnup when enrichment of the feed fuel is assumed fixed. This formulation is meaningful and natural to see the effect of the optimal control rod programming. However, this is not suitable to see its effect under the requirement that the refueling interval should be one year (or some other fixed period of time). It is necessary to fix the average discharge burnup and minimize the enrichment of the feed fuel. In the following discussion, similar to that in Sec. V, however, the above two problems are shown to be equivalent.

It is assumed that the enrichment dependence of the depletion coefficient of the fuel characteristics is small compared to that of the initial fuel characteristics. This is justified by the fact that $|a\alpha| \ll \gamma$ (Sec. IV).

Let the initial and the final states corresponding to the optimal control rod programming for a fixed enrichment be denoted as σ_i^0 and σ_f^0. Assume that the same discharge burnup can be attained by the smaller enrichment. From Eqs. (33) and (34), and with the above assumption, the following variational equations must hold

1. out-in scheme

$$\delta\sigma_{1i} = \frac{N_1 - 1}{N_1 + 1}\,\delta\sigma_{1f} + \frac{4N_2}{(N_1 + 1)(N_2 + 1)}\,\delta\sigma_{2f} - \frac{2(N_2 - 1)}{(N_1 + 1)(N_2 + 1)}\,\gamma\,\delta\eta$$

$$\delta\sigma_{2i} = \frac{N_2 - 1}{N_2 + 1}\,\delta\sigma_{2f} + \frac{2\gamma}{N_2 + 1}\,\delta\eta$$

$$N_1\delta\sigma_{1f} - \frac{N_2(N_1 - 1)}{N_2 + 1}\,\delta\sigma_{2f} - \frac{N_1 + N_2}{N_1 + 1}\,\gamma\delta\eta = 0 \qquad (41)$$

2. in-out scheme

$$\delta\sigma_{1i} = \frac{N_1 - 1}{N_1 + 1}\,\delta\sigma_{1f} + \frac{2\gamma}{N_1 + 1}\,\delta\eta$$

$$\delta\sigma_{2i} = \frac{4N_1}{(N_1 + 1)(N_2 + 1)}\,\delta\sigma_{1f} + \frac{N_2 - 1}{N_2 + 1}\,\delta\sigma_{2f} - \frac{2(N_1 - 1)}{(N_1 + 1)(N_2 + 1)}\,\gamma\delta\eta$$

$$N_2\delta\sigma_{2f} - \frac{N_1(N_2 - 1)}{N_1 + 1}\,\delta\sigma_{1f} - \frac{N_1 + N_2}{N_1 + 1}\,\gamma\delta\eta = 0 \qquad (42)$$

3. parallel scheme

$$\delta\sigma_{1i} = \frac{N_1 - 1}{N_1 + 1}\,\delta\sigma_{1f} + \frac{2\gamma}{N_1 + 1}\,\delta\eta$$

$$\delta\sigma_{2i} = \frac{N_2 - 1}{N_2 + 1}\,\delta\sigma_{2f} + \frac{2\gamma}{N_2 + 1}\,\delta\eta$$

$$\frac{v_1}{N_1 + 1}\,\delta\sigma_{1f} + \frac{v_2}{N_2 + 1}\,\delta\sigma_{2f} - \left(\frac{v_1}{N_1 + 1} + \frac{v_2}{N_2 + 1}\right) \times \gamma\delta\eta = 0\ . \qquad (43)$$

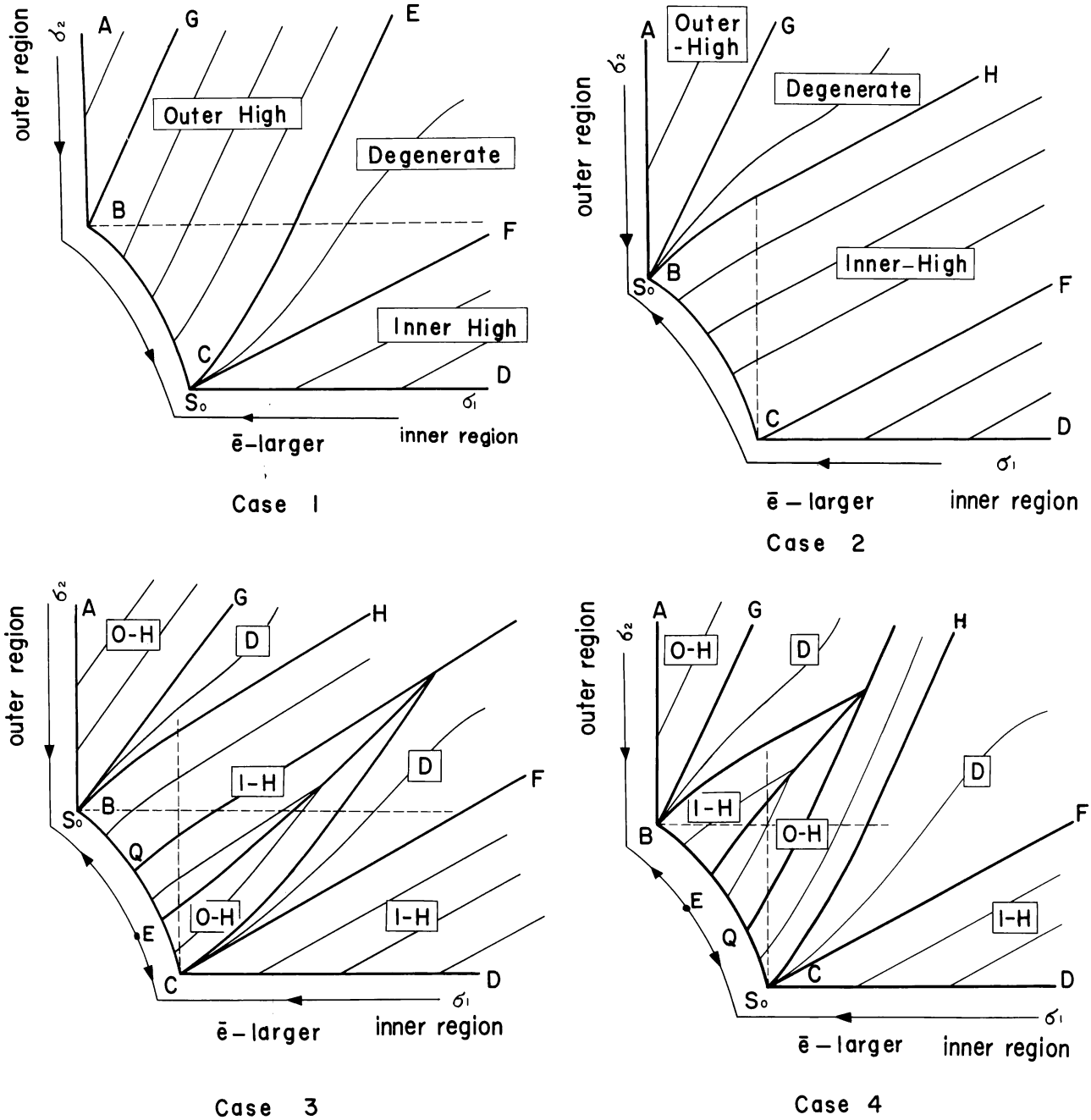

Fig. 15. Synthesis of optimal control for parallel scheme.

The third equation of each refueling scheme shows that the final state must move along the target curve toward larger burnup which is given in case of the fixed enrichment. The method of the proof is essentially the same as that given in Sec. V. An added condition is that $\delta\eta < 0$. From Eqs. (41) through (43), the following relations are obtained which determine the range of the variations of the initial states

1. out-in scheme

$\delta\sigma_{1i} > 0, \quad \delta\sigma_{2i} < \delta\sigma_{2f}, \quad \delta\sigma_{2f} > 0$

region $\gamma\alpha\beta$ Case a

$\delta\sigma_{1f} < \delta\sigma_{1i}, \quad \delta\sigma_{1f} < 0, \quad \delta\sigma_{2i} < \delta\sigma_{2f}, \quad \delta\sigma_{2f} > 0$

region $\gamma\alpha\xi$ Case b

$\delta\sigma_{1f} < \delta\sigma_{1f}, \quad \delta\sigma_{1f} < 0, \quad \delta\sigma_{2i} < 0$

region $\gamma\alpha\beta$ Case c

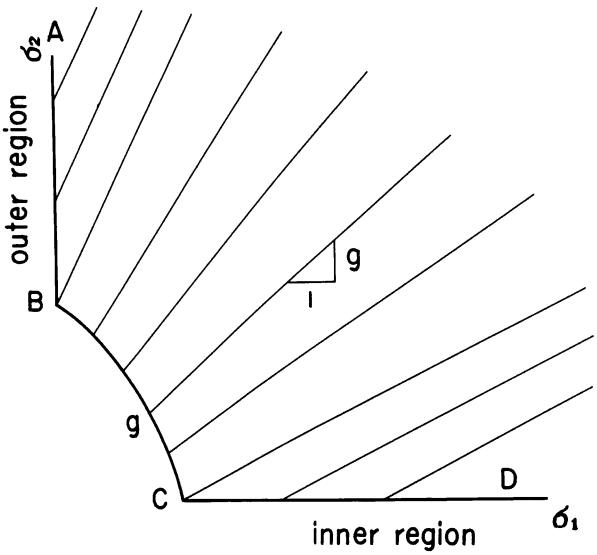

Fig. 16. Synthesis of control by constant power shape operation.

2. in-out scheme

$\delta\sigma_{1i} < 0, \quad \delta\sigma_{2f} < \delta\sigma_{2i}, \quad \delta\sigma_{2f} < 0$

region $\gamma\alpha\beta$ Case a

$\delta\sigma_{1i} < \delta\sigma_{1f}, \quad \delta\sigma_{1f} > 0, \quad \delta\sigma_{2f} < \delta\sigma_{2i}, \quad \delta\sigma_{2f} < 0$

region $\gamma\alpha\xi$ Case b

$\delta\sigma_{1i} < \delta\sigma_{1f}, \quad \delta\sigma_{1f} > 0, \quad \delta\sigma_{2i} > 0$

region $\gamma\alpha\beta$ Case c

3. parallel scheme

$\delta\sigma_{1i} < 0, \quad \delta\sigma_{2f} < \delta\sigma_{2i} < 0$

region $\gamma\alpha\sigma_i^0\beta$ Case a

$\delta\sigma_{1f} < \delta\sigma_{1i} < 0, \quad \delta\sigma_{2i} < \delta\sigma_{2f}, \; \delta\sigma_{2f} > 0$

region $\zeta\gamma\alpha\xi$ Case b

$\delta\sigma_{1i} < \delta\sigma_{1f}, \quad \delta\sigma_{1f} > 0, \quad \delta\sigma_{2f} < \delta\sigma_{2i} < 0$

region $\zeta\gamma\alpha\xi$ Case c

$\delta\sigma_{1f} < \delta\sigma_{1i} < 0, \quad \delta\sigma_{2i} < 0$

region $\gamma\alpha\sigma_i^0\beta$ Case d .

The following relations are used for the parallel scheme in deriving the above inequalities

$$\delta\sigma_{1i} = \frac{v_1(N_1+1)(N_2+1) + v_2(N_1+1)(N_1-1)}{v_1(N_1+1)(N_2+1) + v_2(N_1+1)^2}\,\delta\sigma_{1f} + \frac{2v_2}{v_1(N_2+1) + v_2(N_1+1)}\,\delta\sigma_{2f}$$

$$\delta\sigma_{2i} = \frac{v_1(N_2+1)(N_2-1) + v_2(N_1+1)(N_2+1)}{v_1(N_2+1)^2 + v_2(N_1+1)(N_2+1)}\,\delta\sigma_{2f} + \frac{2v_1}{v_1(N_2+1) + v_2(N_1+1)}\,\delta\sigma_{1f} \quad .$$

These regions are shown in Figs. 10 through 13 as the sum of the two shaded regions of lines with negative and positive gradients. It is evident that these regions are outside the attainable region Γ. When σ_i^0 is the optimal terminal state, the third expression of Eq. (43) cannot be satisfied unless the constraint on the power-peaking factor is moderated. Thus, it is proved for each scheme that the same discharge burnup cannot be attained by the smaller enrichment and the problems are equivalent.

VII. RESULTS

Numerical calculations were performed for each proposed refueling scheme listed in Table II. Although it is possible to find the solution satisfying an equilibrium condition directly, an alternative method is adopted here. The optimal policy was applied repeatedly as a synthesis problem starting from an initial core using synthesis trajectories in Figs. 13, 14, and 15, until the equilibrium condition was satisfied. These trajectories are optimal only when applied in the equilibrium cycle. Therefore, the calculated trajectories in the transient cycles have no definite meaning, nor are they optimal. However, this procedure is useful in understanding how equilibrium is established. Optimal control rod programming in an equilibrium fuel cycle was obtained first by assuming an enrichment and, next, minimum enrichment was obtained so that the maximum discharge burnup obtained became equal to the required value. The same process was taken for a constant power shape operation and both results were compared.

The maximum allowable power-peaking factor was set at 1.40 for all refueling schemes. This value is probably large as a gross radial power-peaking factor compared with the actual design limit; however, the one-group treatment requires this large a value to obtain the freedom of controlling the power shape.

The results are listed in Tables III and IV. The refueling schemes are arranged in order of increasing enrichment of the first ten refueling schemes for each refueling fraction. Table III refers to the refueling fraction 0.25 or the average discharge burnup of 22 GWd/T and Table IV refers to that of 0.2 or 27.5 GWd/T. The maximum discharge burnup is also shown when the enrichment is fixed at 2.65% for reference. Trajectories in burnup space corresponding to the

TABLE III

Comparison of Results (Refueling Fraction = 0.25)

				$\bar{e}$ = 22.0 GWd/T							η = 2.65%		
J	N_1	N_2	v_1	η_1	η_2	$\Delta\eta$	e_1	e_2	Rod[a]	Policy	$\bar{e}_1$	$\bar{e}_2$	$\Delta\bar{e}$
0	4	4	1/3	2.159	2.184	0.025	24.02	20.90	out	O-H	27.91	27.65	0.26
0	3	5	3/8	2.191	2.191	0.000	22.06	21.93	1 in (~0)	I-H	27.82	27.82	0.00
0	4	4	1/2	2.213	2.243	0.030	24.48	19.51	out	D	27.34	26.91	0.43
1	3	1	3/4	2.262	2.279	0.017			out	I-H	26.68	25.98	0.70
0	4	4	2/3	2.326	2.326	0.000	25.86	14.58	1 in (~0)	I-H	25.96	25.96	0.00
0	5	3	5/8	2.411	2.450	0.039	28.63	15.40	out	O-H	24.77	24.30	0.47
1	2	2	1/2	2.432	2.515	0.083			2 in	I-H	23.95	23.14	0.81
0	3	6	1/2	2.460	2.460	0.000	20.08	24.30	1 in	I-H	24.22	24.22	0.00
0	6	3	1/2	2.525	2.525	0.000	33.30	16.37	2 in	O-H	23.03	23.03	0.00
0	2	6	1/4	2.542	2.542	0.000	15.52	28.50	1 in	I-H	23.08	23.08	0.00

η_1 = enrichment % (optimal control)
η_2 = enrichment % (constant shape)
$\Delta\eta = \eta_2 - \eta_1$
e_1 = discharge burnup of the inner region GWd/T (optimal control)
e_2 = discharge burnup of the outer region GWd/T (optimal control)
$\bar{e}_1$ = average discharge burnup GWd/T (optimal control)
$\bar{e}_2$ = average discharge burnup GWd/T (constant shape)
$\Delta\bar{e} = \bar{e}_1 - \bar{e}_2$
[a]Control rod at the final state.

optimal control rod programming and the constant power shape operation are shown in Fig. 17, a through e, for some of the refueling schemes, and the effect of the refueling and the control rod programming on the required enrichment is illustrated in Fig. 18.

As made clear in Sec. V, the optimal control rod programming depends on the refueling scheme in question. Numerical results for parallel schemes show that the optimal policy is degenerate for three schemes [4-4(1/2), 4-6(2/5), 5-5(1/2)], outer high for five schemes [4-4(1/3), 5-3(5/8), 6-3(1/2), 5-5(1/3), 6-4(3/5)], and inner high for seven schemes [3-5(3/8), 3-6(1/2), 4-4(2/3), 2-6(1/4), 5-5(2/3), 3-6(1/5), 6-3(4/5)]. Control rods are fully withdrawn for the first two policies except for the 6-3(1/2) scheme which ranks next to last, and the inner rods are still inserted for the third policy.

Therefore, it is concluded that it is best for the practical range of parallel schemes to try to reach the optimal terminal state C at which the reactor can be critical with minimum total buckling and the power distribution is MAIHD, although the true optimal terminal state, defined as the state where the average discharge burnup is maximum, may occur at B (Fig. 15). In other words, the region around the state B on the target curve is unattainable in equilibrium.

Power distribution is kept constant throughout the reactor life for some refueling schemes. This occurs when the converged initial state is within the regions ABG and FCD in Figs. 13, 14, and 15, and the control rod of either region still has to be inserted at the end state. In this case there is no difference between the operation by optimal control rod programming and by constant power shape. The eight schemes fall in this case: one parallel 6-3(1/2) with outer high policy and seven parallel schemes with inner high policy. Among

TABLE IV

Comparison of Results (Refueling Fraction = 0.20)

				$\bar{e}$ = 27.5 GWd/T							η = 2.65%		
J	N_1	N_2	v_1	η_1	η_2	$\Delta\eta$	e_1	e_2	Rod	Policy	$\bar{e}_1$	$\bar{e}_2$	$\Delta\bar{e}$
0	4	6	2/5	2.510	2.522	0.012	28.19	26.84	out	D	29.25	29.08	0.17
0	5	5	1/3	2.525	2.546	0.021	29.92	26.30	out	O-H	29.05	28.80	0.25
0	5	5	1/2	2.571	2.607	0.036	30.07	24.95	out	D	28.48	28.02	0.46
0	5	5	2/3	2.685	2.685	0.000	31.69	19.13	1 in (~0)	I-H	27.05	27.05	0.00
0	3	6	1/5	2.698	2.698	0.000	25.60	34.90	1 in	I-H	26.87	26.87	0.00
0	6	4	3/5	2.743	2.777	0.034	34.03	20.98	out	O-H	26.36	25.93	0.43
1	4	1	4/5	2.762	2.762	0.000			out	I-H	19.98	19.98	0.00
1	3	2	3/5	2.782	2.905	0.123			2 in	I-H	26.19	25.10	1.09
1	2	3	2/5	3.129	3.226	0.097			2 in	O-H	23.36	22.72	0.64
0	6	3	4/5	3.179	3.179	0.000	39.66	10.81	1 in	I-H	10.00	10.00	0.00

them, parallel 3-5(3/8) ranks second. Although the rods are still inserted at the end in this scheme, they are almost withdrawn, as seen in Fig. 17c. From these results, it cannot be concluded that the operation of constant power shape is always behind the optimal solution.

In general, it is disadvantageous to terminate the operation while the control rods are still in the core. However, whether all the control rods can be fully withdrawn or not is mainly determined by the refueling scheme rather than by the control rod programming.

In series schemes, it is better that the control rods remain inserted even at the end (outer rods for out-in scheme and inner rods for in-out scheme), as explained in Sec. V, contrary to common sense. However, the power shape is not constant in this case. The three schemes out-in 1-2(1/2), 3-2(3/5), 2-3(2/5) fall in this case.

The differences between the optimal solution and the operation of constant power shape range 1 to 4% in the necessary enrichment or the attained burnup for the refueling schemes considered in the present study, but most of them are within 2%.

Note that the refueling schemes with degenerate policy rank high and are promising. These are parallel 4-4(1/2), 4-6(2/5), and 5-5(1/2). No unique policy exists in this case. For an operator, this policy can be thought preferable to other unique optimal policies and the policy of constant power shape operation, because the freedom of operation is left in this policy and the control rod programming can be corrected when the trajectory deviates from the planned course. In other unique policies, however small the deviation may be, it is impossible to put the trajectory back on its right course. Moreover, it is also possible to optimize other performance indexes using this freedom. Trajectories of this policy, shown in Figs. 17b and c, are selected such that they are tangent to the upper boundary curve entering into the optimal terminal state C. The operation along these trajectories is similar to the outer high policy in that the power shape is constant until the outer rods are fully withdrawn. This selected operation, of course, gives a larger burnup than the operation of constant power shape.

Tables III and IV and Fig. 18 show, in general, that the differences in enrichment or burnup among the different refueling schemes are much larger than those among the rod programmings.

The difference between the refueling schemes that rank first and second is 1.5% in enrichment and 0.31% in burnup in Table III and 0.6% and 0.7% in Table IV. This difference is small and comparable to that introduced by control rod programming. However, the difference between the the first and the fifth amounts to about 7% in Table III and 8% in Table IV, both in enrichment and

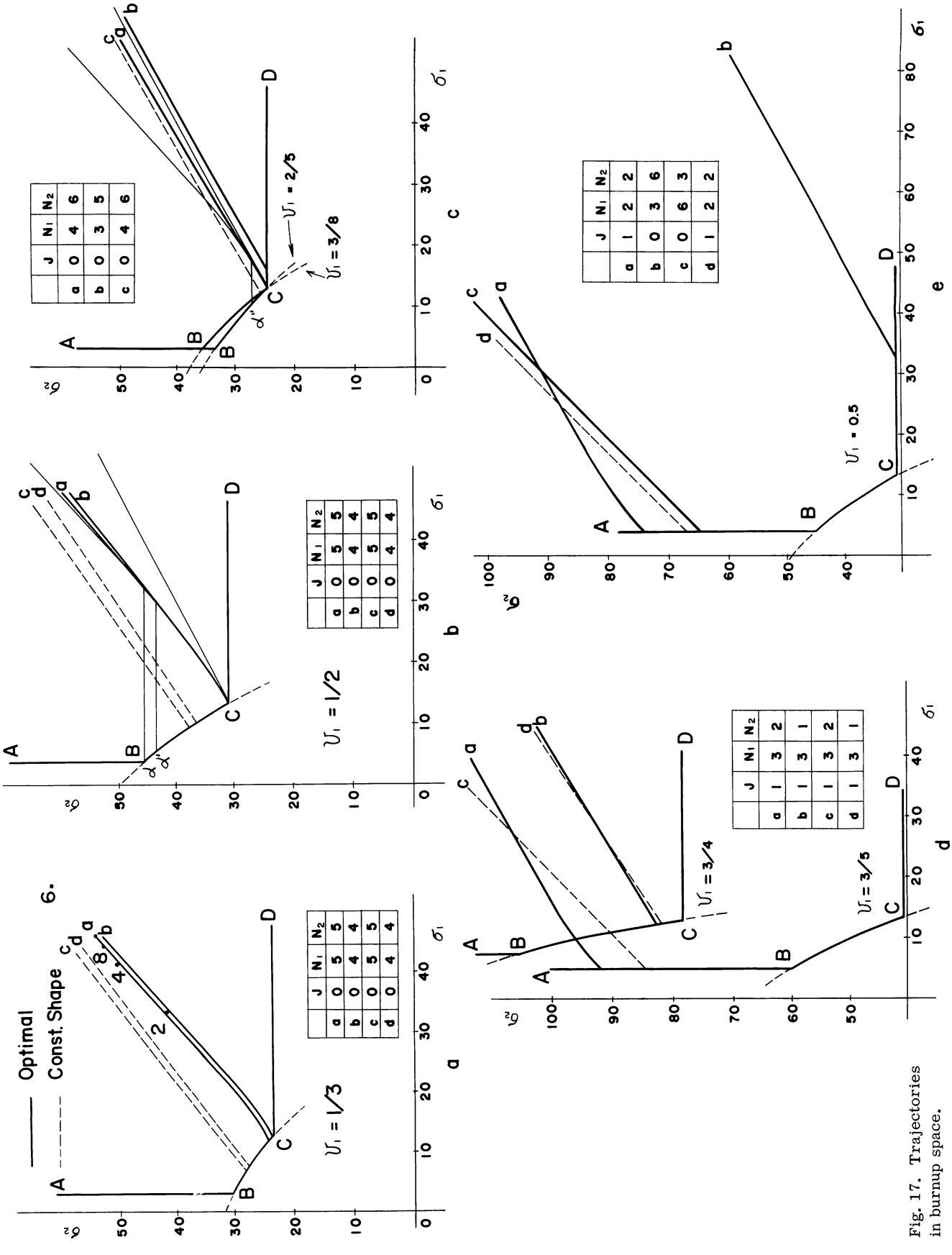

Fig. 17. Trajectories in burnup space.

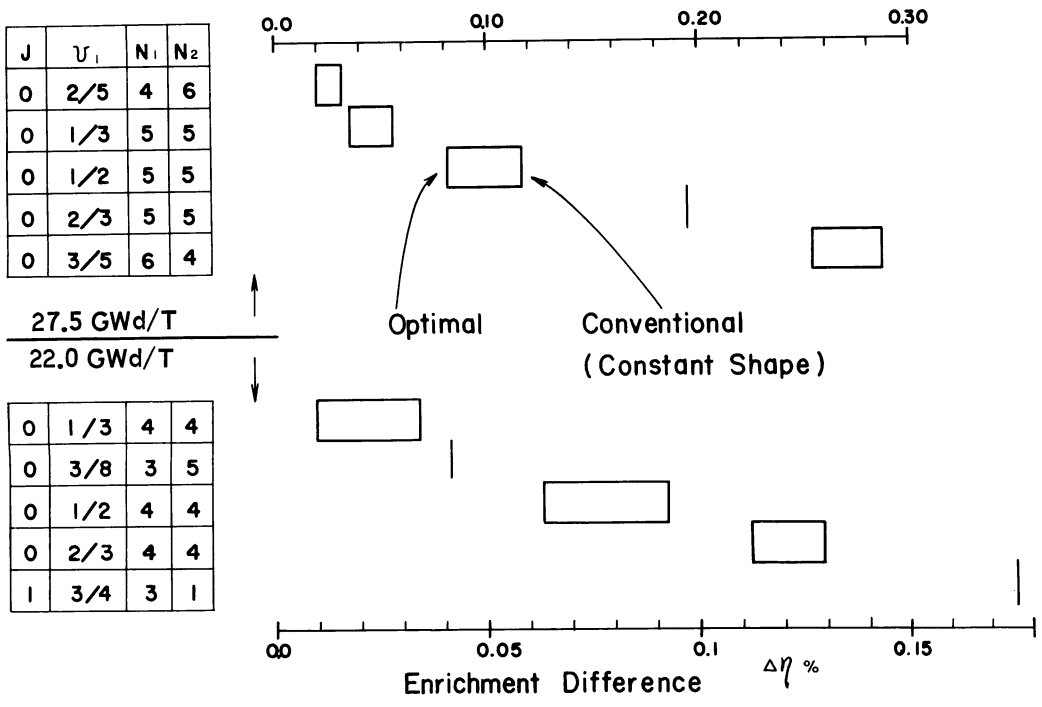

Fig. 18. Effect of refueling and rod programming.

burnup; the difference between the first and the tenth (the last) amounts to as much as 20% in both in Table III; 25% in enrichment, and 65% in burnup in Table IV.

The differences in enrichment or burnup among the different control rod programmings are comparable only to those of the first three refueling schemes and the difference of the first and fifth is about four times larger than the differences introduced by the control rod programmings. This result is natural from the hierarchy relation of these two problems. Therefore, the refueling scheme should be first optimized as done in previous works.[1,3,6]

The optimal control rod programming was compared only with the operation at constant power shape. It is possible to compare it with other rod programmings such as uniform control; however, this programming is worse than the rod programming of constant power shape operation, as shown in Ref. 13.

The present analysis indicates that the promising refueling schemes are parallel 4-4(1/3) and 3-5(3/8) for a refueling fraction of 0.25 and parallel 4-6(2/5) and 5-5(1/3) for a refueling fraction of 0.20. It is shown that the uniform scatter loading is not optimal in Stover's[3] paper where the core is divided into three regions. The purpose of the present paper is to find the policy of optimal control rod programming and not to discuss in detail the features of optimal refueling schemes, for which the present model has to be greatly improved. However, the following conclusion can be drawn. The batch number of the outer region should not be less than that of the inner region ($N_1 \leq N_2$), which increases the uniformity of the discharge burnup of both regions. This characteristic will hold even when the constraint on the maximum allowable discharge burnup is accounted for, which is not done in this study. Also note that the refueling schemes with the smaller volume fraction of the inner region rank higher when the batch numbers of both regions are equal. This means that a more uniform burnup distribution is obtained when the shuffling region in the outer region is wider. This effect is seen in Tables III and IV.

The out-in schemes are not as promising as expected. This scheme is unfavorable from a viewpoint of fuel importance because the new fuels are always loaded in the outer region where the fuel importance is generally smaller than in the inner region. Moreover, it seems that series schemes are intrinsically inferior to parallel schemes in that the higher burnup is attained when the reactor terminates operation with the control rods still in the core.

No in-out schemes are listed in Tables III and IV. No equilibrium condition exists for these schemes. This is mainly because the limit of the

power-peaking factor of 1.4 is too severe for these schemes, considering that the new fuels are loaded in the inner region, which necessitates a higher power density of the inner region. In almost all cases it turns out that $\sigma_{2i} < \sigma_{2f}$. Therefore, this scheme is neither good nor practical.

The difference between the optimal control rod programming and the constant power shape operation is large for out-in schemes where the outer rods still have to be inserted in the core at the end. This is because the control freedom of power distribution is fully used from MAIHD to MAOHD in the optimal solution, whereas the power distribution is fixed at MAOHD in the constant power shape operation.

The equivalent relation proved in Sec. VI does not necessarily mean that for every specified rod programming the ranking of the refueling schemes when the enrichment is fixed is always equal to the ranking when the discharge burnup is fixed. In other words, the ranking is affected by the required discharge burnup or by the enrichment of the feed fuel. This comes from the fact that the enrichment dependence of the discharge burnup is different from each refueling scheme and each rod programming. Actually, the parallel schemes 4-4(1/3) and 3-5(3/8) in Table III are reversed in order of burnup for constant power shape operation. This comes from the difference in the value of the power-peaking factor. Operation at constant power shape, in which all of the control rods can be withdrawn at the end, is optimal in the sense that the worst power-peaking factor during the operation period is minimum as far as the two-region model is valid. The peaking factor of the parallel scheme 4-4(1/3) is 1.37, while in the parallel scheme 3-5(3/8) it is 1.40. From a different standpoint, the former scheme can be thought to be under a more severe constraint on the power-peaking factor. The out-in 4-1(4/5) scheme in Table IV should rank next to the last in order of burnup. Control rods in the inner region are still inserted when the enrichment is 2.65%, while they are completely withdrawn when it is 2.762%. In this range of the enrichment, $\Delta e/\Delta\eta$ is very large for this scheme. Similar consideration is applied to other refueling schemes. Therefore, the rankings may be used as a guide for fuel management evaluations.

The approach to equilibrium is shown in Fig. 17a for parallel scheme 5-5(1/3). Only the initial states of selected cycles are plotted. At least several cycles, i.e., several years, are necessary to reach equilibrium within the error of several percent. The optimization of the transient cycles is also an important subject, but it is outside of this work.

VIII. CONCLUSIONS

The nature of the optimal control rod programming in various refueling schemes is investigated for a single enrichment two-region BWR. It is very convenient to interpret the relations among power shape, fuel burnup, criticality, and control rod programming as the geometical relation in the burnup space.

First, optimal control programming was solved to maximize the average discharge burnup in an equilibrium fuel cycle for a reactor with fixed fuel enrichment. This problem was then shown to be equivalent to minimizing the enrichment of the feed fuels for a reactor with fixed discharge burnup. This facilitates incorporating the requirement of a one-year refueling interval. The following conclusions are obtained by these analyses:

1. The policy of optimal control rod programming is made clear. It strongly depends on the refueling scheme adopted; for example

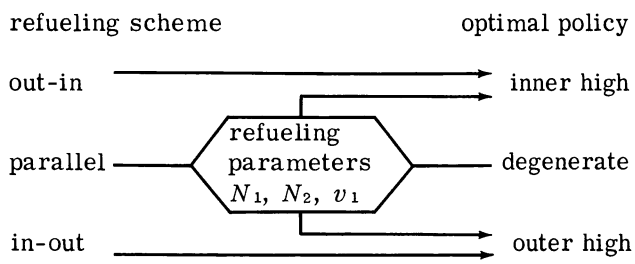

2. All the control rods should be fully withdrawn at the end of the operation for the parallel scheme. However, some of the control rods should remain in the core for the series scheme: outer rods for the out-in scheme and inner rods for the in-out scheme. Whether this condition is satisfied or not is mainly determined by refueling parameters rather than by control rod programming.

3. The optimal refueling scheme should be chosen from parallel schemes, which have larger freedom than series schemes. Out-in schemes are not as advantageous as expected. In-out schemes are almost hopeless because of their very poor power distribution.

4. Optimal control rod programming for the practical range of parallel schemes is to arrive as nearly as possible at the state at which the reactor becomes critical with minimum material buckling. The power distribution at this state is the maximum allowable in the inner high.

5. The promising refueling schemes found among parallel schemes are

4-4(1/3), 3-5(3/8)	refueling fraction 0.25
4-6(2/5), 5-5(1/3)	refueling fraction 0.20.

In general, batch numbers in the outer region should not be less than those in the inner region, and fuel assemblies should be shuffled or mixed in the wider outer region.

6. The difference in the required enrichment or the attained discharge burnup amounts to more than 20% between the best and the worst refueling schemes, while the differences between the optimal control rod programming and nonoptimal one (constant power shape operation) is at most only 4%. This is natural in view of the hierarchy relation between the fuel management and the poison management. However, the differences among the promising refueling schemes are comparable to those among control rod programmings. In general, the refueling scheme should be optimized first.

7. For some refueling schemes operation of constant power shape becomes optimal. Parallel scheme 3-5(3/8) falls in this case and ranks second. Whether this situation will occur strongly depends on the refueling parameters.

8. A degenerate policy is optimal for some of the promising parallel schemes: 4-4(1/2), 4-6(2/5), and 5-5(1/2). This policy has two advantages over the unique policies. One is that the control rod programming can be modified to reach the optimal terminal state if it happens that the trajectory deviates from the planned course. Another is that is is possible to optimize other performance indexes using the freedom of operation while ensuring maximum burnup.

9. If the optimal control rod programming is unique, it is bang pang control in which either the power peaking takes its maximum allowable value or the density of the control rods takes its minimum value. In general, the optimal condition is in conflict with the safety margin and a qualitative evaluation of the safety criteria is necessary.

10. The ranking of refueling schemes is affected by the enrichment of feed fuels or the required discharge burnup. The value of the maximum allowable power-peaking factor is fixed at 1.4 in this study, which can be thought as an important design parameter. The difference between the optimal control rod programming and the constant power shape operation is also affected by this quantity, which may even result in a different policy in parallel schemes. Therefore, the dynamic optimization is inevitably necessary at the design stage so that the optimal control rod programming and the optimal refueling schedule can be determined, as well as the optimal values of the design parameters. The rankings obtained in this study should be regarded as a guide for fuel management evaluations.

The above conclusions, which are very intuitive and clear, are based on a very simple, one-dimensional, one-group, two-region model. This precludes effects of void feedback, nonuniform axial distribution of control rods in a region, local power peaking, and fuel burnout, etc. These take a very important place in the actual reactor operation. Extension to the three-dimensional, multigroup multiregion core treatment, which includes these microscopic constraints, is necessary to make sure of the above results, to make a more quantitative evaluation, and to find a rule for the three-dimensional assignment of the finite numbers of the control rods. Direct extension of the present method of analysis will be very difficult because the concept of the control of the trajectory will no longer be intuitive, and the application of mathematical programming, such as the method of approximate programming,[15] will be useful.

The optimal control rod programming considered in this paper is not disadvantageous from an operational viewpoint. It will be possible in the near future for a process computer to take the place of the operator and determine the optimal sequence of withdrawal of control rods at each instant from the present state of the reactor.

ACKNOWLEDGMENTS

The author is deeply indebted to K. Taniguchi and S. Yamada for their encouragement throughout this work, to T. Kawai for his many valuable suggestions, and K. Fukunishi for his help in numerical calculations. He also extends his appreciation to T. Kiguchi and M. Senoo for many useful discussions, and J. M. Clary for reading this manuscript.

[15]R. E. GRIFFITH and R. A. STEWART, *Management Sci.*, **7**, 379 (1961).